

The new $(g - 2)_\mu$ result and the $\mu\nu$ SSM

Sven Heinemeyer^{*a,b,c}, Essodjolo Kpatcha^{†a,d}, Iñaki Lara^{‡e},
Daniel E. López-Fogliani^{§f,g}, Carlos Muñoz^{¶a,d}, and Natsumi Nagata^{||h}

^a*Instituto de Física Teórica (IFT) UAM-CSIC, Campus de Cantoblanco, 28049 Madrid, Spain*

^b*Campus of International Excellence UAM+CSIC, Cantoblanco, 28049, Madrid, Spain*

^c*Instituto de Física de Cantabria (CSIC-UC), 39005, Santander, Spain*

^d*Departamento de Física Teórica, Universidad Autónoma de Madrid (UAM), Campus de Cantoblanco, 28049 Madrid, Spain*

^e*Faculty of Physics, University of Warsaw, Pasteura 5, 02-093 Warsaw, Poland*

^f*Instituto de Física de Buenos Aires UBA & CONICET, Departamento de Física, Facultad de Ciencia Exactas y Naturales, Universidad de Buenos Aires, 1428 Buenos Aires, Argentina*

^g*Pontificia Universidad Católica Argentina, Av. Alicia Moreau de Justo 1500, 1107 Buenos Aires, Argentina*

^h*Department of Physics, University of Tokyo, Tokyo 113-0033, Japan*

Abstract

The $\mu\nu$ SSM is a highly predictive alternative model to the MSSM. In particular, the electroweak sector of the model can explain the longstanding discrepancy between the experimental result for the anomalous magnetic moment of the muon, $(g - 2)_\mu$, and its Standard Model prediction, while being in agreement with all other theoretical and experimental constraints. The recently published MUON G-2 result is within 0.8σ in agreement with the older BNL result on $(g - 2)_\mu$. The combined result was announced as $a_\mu^{\text{exp}} = (11659206.1 \pm 4.1) \times 10^{-10}$, yielding a new deviation from the Standard Model prediction of $\Delta a_\mu = (25.1 \pm 5.9) \times 10^{-10}$, corresponding to 4.2σ . Using this improved bound we update the analysis in the $\mu\nu$ SSM as presented in Ref. [1] and set new limits on the allowed parameters space of the electroweak sector of the model. We conclude that significant regions of the model can explain the new $(g - 2)_\mu$ data.

IFT-UAM/CSIC-21-034

*Sven.Heinemeyer@cern.ch

†kpatcha.essodjolo@uam.es

‡inaki.lara@fuw.edu.pl

§daniel.lopez@df.uba.ar

¶c.munoz@uam.es

||natsumi@hep-th.phys.s.u-tokyo.ac.jp

1 Introduction

The experimental result for the anomalous magnetic moment of the muon, $a_\mu := \frac{1}{2}(g-2)_\mu$, was so far dominated by the measurements made at Brookhaven National Laboratory (BNL) [2], resulting in a world average of [3]

$$a_\mu^{\text{exp-BNL}} = (11659209.1 \pm 6.3) \times 10^{-10}, \quad (1)$$

combining statistical and systematic uncertainties. The Standard Model (SM) prediction of a_μ is given by [4] (based on Refs. [5–24]),

$$a_\mu^{\text{SM}} = (11659181.0 \pm 4.3) \times 10^{-10}, \quad (2)$$

corresponding to a 3.7σ discrepancy.

Recently, the MUON G-2 collaboration [25] published the results (referred to as “FNAL” result) of their Run 1 data [26],

$$a_\mu^{\text{exp-FNAL}} = (11659204.0 \pm 5.4) \times 10^{-10}, \quad (3)$$

being within 0.8σ well compatible with the previous experimental result in Eq. (1). The combined experimental result was announced as

$$a_\mu^{\text{exp}} = (11659206.1 \pm 4.1) \times 10^{-10}. \quad (4)$$

Compared with the SM prediction in Eq. (2), this yields a new deviation of

$$\Delta a_\mu = (25.1 \pm 5.9) \times 10^{-10}, \quad (5)$$

corresponding to a 4.2σ discrepancy.

In Ref. [1], some of us performed an analysis of the (then current) deviation of a_μ [5, 6], taking into account all relevant data for the electroweak (EW) sector of the ‘ μ from ν ’ Supersymmetric Standard Model ($\mu\nu$ SSM) [27] (for a recent review of the model, see Ref. [28]). The experimental results imposed comprise (as will be detailed in Sect. 2) Higgs and neutrino data, flavor observables such as B and μ decays, as well as the direct searches at the LHC [29–36]. Sampling the $\mu\nu$ SSM, it was analyzed which parameter (combinations) are favored by a_μ measurements. It was found that the $\mu\nu$ SSM can naturally produce moderately light left-handed muon-sneutrinos ($120 \text{ GeV} \lesssim m_{\tilde{\nu}_\mu} \lesssim 620 \text{ GeV}$) and wino-like charginos ($200 \text{ GeV} \lesssim m_{\tilde{W}^\pm} \lesssim 930 \text{ GeV}$), accommodating the discrepancy between experimental and SM values. A recent general analysis in the Minimal Supersymmetric Standard Model (MSSM) [37–41] can be found in Refs. [42, 43].

In this work, we analyze the combination of the FNAL Run 1 data with the previous BNL result. Using this improved bound we update the results presented in Ref. [1] and set new limits on the allowed parameters space of the EW sector of the $\mu\nu$ SSM, as shown in Figs. 7 and 8 to be discussed below. The results will be discussed in the context of searches for EW particles at the LHC and future colliders. A recent general analysis of the impact of the new FNAL result in the MSSM can be found in Ref. [44].

2 The model and the experimental constraints

2.1 The $\mu\nu$ SSM and a_μ

In the $\mu\nu$ SSM [27, 28], the particle content of the MSSM is extended by right-handed neutrino superfields $\hat{\nu}_i^c$ ($i = 1, 2, 3$). In the early universe not only the EW symmetry is broken, but in addition to the neutral components of the Higgs doublet fields H_d and H_u also the left-handed (LH) and right-handed (RH) scalar neutrinos $\tilde{\nu}_i$ and $\tilde{\nu}_{iR}$ acquire a vacuum expectation value (vev). With the choice of CP conservation, they develop the following real vevs:

$$\langle H_d^0 \rangle = \frac{v_d}{\sqrt{2}}, \quad \langle H_u^0 \rangle = \frac{v_u}{\sqrt{2}}, \quad \langle \tilde{\nu}_{iR} \rangle = \frac{v_{iR}}{\sqrt{2}}, \quad \langle \tilde{\nu}_i \rangle = \frac{v_i}{\sqrt{2}}. \quad (6)$$

The EW symmetry breaking is induced by the soft supersymmetry (SUSY)-breaking terms of $\mathcal{O}(1 \text{ TeV})$, and therefore also $v_{iR} \sim \mathcal{O}(1 \text{ TeV})$. Since $\tilde{\nu}_{iR}$ are gauge-singlet fields, the μ -problem can be solved in total analogy to the Next-to-MSSM (NMSSM) [45, 46] through the presence of trilinear terms in the superpotential involving RH neutrinos ν_{iR} , $\lambda_i \hat{\nu}_i^c \hat{H}_d \hat{H}_u$, where the summation convention is implied on repeated indices. Then, the value of the effective μ -parameter is given by $\mu = \lambda_i v_{iR} / \sqrt{2}$. These trilinear terms also relate the origin of the μ -term to the origin of neutrino masses and mixing angles, since Yukawa couplings $Y_{\nu_{ij}} \hat{H}_u \hat{L}_i \hat{\nu}_j^c$ are present in the superpotential generating Dirac masses for neutrinos, $m_{\mathcal{D}_{ij}} \equiv Y_{\nu_{ij}} v_u / \sqrt{2}$. Remarkably, in the $\mu\nu$ SSM it is possible to accommodate neutrino masses and mixings in agreement with experiments [47–50], via an EW seesaw mechanism dynamically generated during the EW symmetry breaking [27, 51–56] through couplings $\kappa_{ijk} \hat{\nu}_i^c \hat{\nu}_j^c \hat{\nu}_k^c$ giving rise to effective Majorana masses for RH neutrinos, $\mathcal{M}_{ij} = 2\kappa_{ijk} \frac{v_{iR} v_{jR}}{\sqrt{2}}$. Actually, this is possible at tree level even with diagonal Yukawa couplings [52, 54], i.e. $Y_{\nu_{ij}} = Y_{\nu_i} \delta_{ij}$.

Therefore, the $\mu\nu$ SSM solves the μ - and the ν -problem (neutrino masses) simultaneously without the need to introduce additional energy scales beyond the SUSY-breaking scale. In contrast to the (N)MSSM, R -parity and lepton number are not conserved, leading to a completely different phenomenology characterized by distinct prompt or displaced decays of the lightest supersymmetric particle (LSP), producing multi-leptons/jets/photons with small/moderate missing transverse energy (MET) from neutrinos [57–60].

The parameter space of the $\mu\nu$ SSM, and in particular the neutrino, neutral Higgs, slepton, chargino and neutralino sectors are relevant for our analysis in order to reproduce neutrino, Higgs and a_μ data. They were discussed in Ref. [1], and we refer the reader to that work for details. Here we summarize the analysis, assuming for simplicity in what follows that the couplings $\lambda_i = \lambda$, $\kappa_{ijk} = \kappa \delta_{ij} \delta_{jk}$, and the vevs $v_{iR} = v_R$. Then, the higgsino mass parameter μ , and Dirac and Majorana masses discussed above are given by:

$$\mu = 3\lambda \frac{v_R}{\sqrt{2}}, \quad m_{\mathcal{D}_i} = Y_{\nu_i} \frac{v_u}{\sqrt{2}}, \quad \mathcal{M} = 2\kappa \frac{v_R}{\sqrt{2}}. \quad (7)$$

Under this assumption, a simplified formula for the effective mass matrix of the light

neutrinos is [54]

$$(m_\nu)_{ij} \approx \frac{m_{\mathcal{D}_i} m_{\mathcal{D}_j}}{3\mathcal{M}} (1 - 3\delta_{ij}) - \frac{v_i v_j}{4M}, \quad \frac{1}{M} \equiv \frac{g'^2}{M_1} + \frac{g^2}{M_2}, \quad (8)$$

where g' , g are the EW gauge couplings, and M_1 , M_2 the bino and wino soft SUSY-breaking masses, respectively. This expression for the mass matrix arises from the generalized EW seesaw of the $\mu\nu$ SSM, where due to R -parity violation (RPV) the neutral fermions have the flavor composition $(\nu_i, \tilde{B}^0, \tilde{W}^0, \tilde{H}_d^0, \tilde{H}_u^0, \nu_{iR})$. One can see that once \mathcal{M} is fixed, as will be done in the parameter analysis of Sec. 3, the most crucial independent parameters determining *neutrino physics* are:

$$Y_{\nu_i}, v_i, M_1, M_2. \quad (9)$$

Note that this EW scale seesaw implies $Y_{\nu_i} \lesssim 10^{-6}$ driving v_i to small values because of the proportional contributions to Y_{ν_i} appearing in their minimization equations in the scalar potential. A rough estimation gives $v_i \lesssim m_{\mathcal{D}_i} \lesssim 10^{-4}$.

In the $\mu\nu$ SSM, the neutral scalars have the flavor composition $(H_d^0, H_u^0, \tilde{\nu}_{iR}, \tilde{\nu}_i)$. However, the LH sneutrinos are basically decoupled from the other states, whereas the doublet-like Higgses and the three RH sneutrinos can be substantially mixed. Neglecting this mixing, the expression of the tree-level mass of the SM-like Higgs is [51]:

$$m_h^2 \approx m_Z^2 (\cos^2 2\beta + 10.9 \lambda^2 \sin^2 2\beta), \quad (10)$$

where $\tan \beta = v_u/v_d$, and m_Z denotes the mass of the Z boson. Effects lowering (raising) this mass appear when the SM-like Higgs mixes with heavier (lighter) RH sneutrinos. The one-loop corrections are basically determined by the third-generation soft SUSY-breaking parameters T_{u_3} , $m_{\tilde{u}_{3R}}$ and $m_{\tilde{Q}_{3L}}$, where T_{u_3} denotes the trilinear parameter in the Lagrangian, $-T_{u_{ij}} H_u \tilde{Q}_{iL} \tilde{u}_{jR}^* + \text{h.c.}$, assuming for simplicity $T_{u_{ij}} = T_{u_i} \delta_{ij}$. These parameters together with the coupling λ and $\tan \beta$, are the crucial ones for Higgs physics. The colored sector is assumed to be heavy and thus beyond the (current) reach of the LHC. This also ensures that the model can contain a scalar boson with a mass around ~ 125 GeV and properties similar to the ones of the SM Higgs boson [61–64].

In addition, κ , v_R and the trilinear parameter T_κ in the soft Lagrangian, $-T_\kappa \tilde{\nu}_{iR}^* \tilde{\nu}_{iR}^* \tilde{\nu}_{iR}^* + \text{h.c.}$, are the key ingredients to determine the mass scale of the RH sneutrino states [51, 52]. For example, for $\lambda \lesssim 0.01$ they are basically free from any doublet admixture, and using their minimization equations in the scalar potential the scalar and pseudoscalar masses can be approximated respectively by [65, 57]:

$$m_{\tilde{\nu}_{iR}}^2 \approx \frac{v_R}{\sqrt{2}} \left(T_\kappa + \frac{v_R}{\sqrt{2}} 4\kappa^2 \right), \quad m_{\tilde{\nu}_{iR}^I}^2 \approx -\frac{v_R}{\sqrt{2}} 3T_\kappa. \quad (11)$$

Finally, λ and the trilinear parameter T_λ in the soft Lagrangian, $-T_\lambda \tilde{\nu}_{iR}^* H_d H_u + \text{h.c.}$, not only contribute to these masses for larger values of λ , but also control the mixing between the singlet and the doublet states and hence, they contribute in determining their mass scales as discussed in detail in Ref. [63]. We conclude that the relevant low-energy

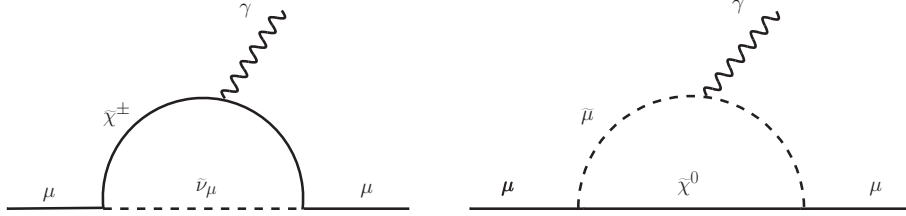


Figure 1: Chargino-LH muon sneutrino (left) and neutralino-smuon (right) one-loop contributions to the anomalous magnetic moment of the muon.

parameters in the *Higgs-RH sneutrino sector* are:

$$\lambda, \kappa, \tan \beta, v_R, T_\kappa, T_\lambda, T_{u_3}, m_{\tilde{u}_{3R}}, m_{\tilde{Q}_{3L}}. \quad (12)$$

We now turn to the SUSY contributions to a_μ . The main contribution to a_μ at the one-loop level in the $\mu\nu$ S $\overline{\text{SM}}$, $a_\mu^{\mu\nu\text{SSM}}$, comes from the diagram involving $\tilde{\chi}^\pm - \tilde{\nu}_\mu$ loops displayed in Fig. 1 (left), similarly to the MSSM. This implies that appropriately decreasing the masses of the LH muon-sneutrino $\tilde{\nu}_\mu$ and charginos $\tilde{\chi}^\pm$ is sufficient to lead to a significant enhancement of a_μ . In addition, as in the MSSM a_μ increases also with increasing $\tan \beta$. The contribution from the diagram involving $\tilde{\chi}^0 - \tilde{\mu}$ loops displayed in Fig. 1 (right), is typically smaller than the $\tilde{\chi}^\pm - \tilde{\nu}_\mu$ one (see e.g. Refs. [66–68]). Nevertheless, we will include in our analysis variations in the masses of neutralinos $\tilde{\chi}^0$ and smuons $\tilde{\mu}$. In this way, $a_\mu^{\mu\nu\text{SSM}}$ could have a further increase for low values of these masses.

Summarizing, for reproducing the value of a_μ we are interested in light charginos, neutralinos, LH muon-sneutrino and smuon, and RH smuon, while the other SUSY particles can be decoupled.

Concerning $\tilde{\chi}^\pm$, they mix with the charged leptons in the $\mu\nu$ S $\overline{\text{SM}}$ but the mixing terms are suppressed, and both type of particles are effectively decoupled. Therefore $\tilde{\chi}^\pm$ are of the MSSM type composed of charged winos and higgsinos, thus $m_{\tilde{\chi}^\pm}$ are determined by M_2 and μ . Note that M_2 is also a crucial parameter for neutrino physics (9), and that μ is not independent parameters as shown in Eq. (7).

As discussed above, $\tilde{\chi}^0$ and ν_{iR} are mixed. As we can see from Eq. (11), a moderate/large negative value of T_κ is necessary to have heavy pseudoscalar RH sneutrinos, but this implies that the value of κ has to be large enough in order to avoid too light (even tachyonic) scalar RH sneutrinos. As a consequence, large Majorana masses (see Eq. (7)) are generated for RH neutrinos. Therefore, the decoupling of RH sneutrinos implies also heavy ν_{iR} , and, in this case, $\tilde{\chi}^0$ are of the MSSM type and composed of neutral EW gauginos and higgsinos. Thus $m_{\tilde{\chi}^0}$ are determined by M_1 , M_2 and μ , where the M_1 parameter is also crucial for neutrino physics.

Concerning smuon masses, in the $\mu\nu$ S $\overline{\text{SM}}$ LH and RH sleptons $\tilde{\ell}_{iL,R}$ are mixed with the charged Higgses, but once again the mixing terms are suppressed and both sectors are essentially decoupled. The same comment applies to the mixing between $\tilde{\ell}_{iL}$ and $\tilde{\ell}_{iR}$ themselves, especially those of the first and second generation because the mixing terms are suppressed by $Y_{e_{ij}}$. Thus $m_{\tilde{\mu}_L}$ and $m_{\tilde{\mu}_R}$ are effectively determined by their soft SUSY-breaking masses $m_{\tilde{L}_{2L}}$ and $m_{\tilde{e}_{2R}}$.

Besides, the masses of $\tilde{\nu}_\mu$ and $\tilde{\mu}_L$ are very similar since these two particles are in the same $SU(2)$ doublet, and therefore both masses are determined by $m_{\tilde{L}_{2L}}$. At the end of the day, $m_{\tilde{\mu}_L}$ is only slightly larger than $m_{\tilde{\nu}_\mu}$ due to the mass splitting produced by the corresponding D -term contributions, $m_{\tilde{\mu}_L}^2 = m_{\tilde{\nu}_\mu}^2 - m_W^2 \cos 2\beta$. Given that $m_{\tilde{L}_{iL}}$ can be determined for the three generations from their minimization equations in the scalar potential, one arrives to the following approximate tree-level expression for the three LH sneutrino masses [51, 52, 57]:

$$m_{\tilde{\nu}_i}^2 \approx \frac{m_{\mathcal{D}_i}}{v_i} v_R \left(\frac{-T_{\nu_i}}{Y_{\nu_i}} - \frac{\mathcal{M}}{2} + \frac{\mu}{\tan \beta} \right), \quad (13)$$

with T_{ν_i} the trilinear parameters in the soft Lagrangian, $-T_{\nu_{ij}} H_u \tilde{L}_{iL} \tilde{\nu}_{jR}^* + \text{h.c.}$, where we take for simplicity $T_{\nu_{ij}} = T_{\nu_i} \delta_{ij}$. Therefore, in addition to the parameters of neutrino and Higgs sectors in Eqs. (9) and (12), *slepton physics* introduces two other independent parameters:

$$T_{\nu_i}, m_{\tilde{e}_{2R}}. \quad (14)$$

From the above discussion, we conclude that of the parameters controlling the SUSY contributions to a_μ , i.e. $M_2, M_1, \mu, m_{\tilde{\nu}_\mu}, m_{\tilde{\mu}_L}, m_{\tilde{e}_{2R}}$ and $\tan \beta$, only

$$M_2, M_1, m_{\tilde{e}_{2R}}, \tan \beta, \quad (15)$$

are independent in this scenario, and besides M_1 and M_2 are also important for neutrino physics and $\tan \beta$ for Higgs physics.

In our analysis of Sec. 4, we will sample the relevant parameter space of the $\mu\nu$ SSM, which contains the independent parameters determining neutrino, Higgs and slepton physics in Eqs. (9), (12) and (14). Given the large number of independent parameters, for our demanding computing task we have employed the **Multinest** [69] algorithm as optimizer. To compute the spectrum and the observables we have used SARAH [70] to generate a **SPheno** [71, 72] version for the model. In this way, we have evaluated the $a_\mu^{\mu\nu\text{SSM}}$ contribution to a_μ .

2.2 Experimental constraints

The a_μ constraint in Eq. (5) was applied at the $\pm 2\sigma$ level. All other experimental constraints (except the LHC searches) are taken into account as follows:

- Neutrino observables

We have imposed the results for normal ordering from Ref. [50], selecting points from the scan that lie within $\pm 3\sigma$ of all neutrino observables. On the viable obtained points we have imposed the cosmological upper bound on the sum of the masses of the light active neutrinos given by $\sum m_{\nu_i} < 0.12$ eV [73].

- Higgs observables

The Higgs sector of the $\mu\nu$ SSM is extended with respect to the (N)MSSM. For constraining the predictions in that sector of the model, we have interfaced **HiggsBounds**

v5.3.2 [74–78] with `Multinest`, using a conservative ± 3 GeV theoretical uncertainty on the SM-like Higgs boson in the $\mu\nu$ SSM as obtained with `SPheno`. (As mentioned above, more refined calculations are possible, but would result only in shifts in the colored sector, which does not play a relevant role in our analysis.). Also, in order to address whether a given Higgs scalar of the $\mu\nu$ SSM is in agreement with the signal observed by ATLAS and CMS, we have interfaced `HiggsSignals` v2.2.3 [79,80] with `Multinest`. We require that the p -value reported by `HiggsSignals` be larger than 5%.

- B decays

$b \rightarrow s\gamma$ occurs in the SM at leading order through loop diagrams. We have constrained the effects of new physics on the rate of this process using the average experimental value of $\text{BR}(b \rightarrow s\gamma) = (3.55 \pm 0.24) \times 10^{-4}$ provided in Ref. [81]. Similarly to the previous process, $B_s \rightarrow \mu^+\mu^-$ and $B_d \rightarrow \mu^+\mu^-$ occur radiatively. We have used the combined results of LHCb and CMS [82], $\text{BR}(B_s \rightarrow \mu^+\mu^-) = (2.9 \pm 0.7) \times 10^{-9}$ and $\text{BR}(B_d \rightarrow \mu^+\mu^-) = (3.6 \pm 1.6) \times 10^{-10}$. We put $\pm 3\sigma$ cuts from $b \rightarrow s\gamma$, $B_s \rightarrow \mu^+\mu^-$ and $B_d \rightarrow \mu^+\mu^-$, as obtained with `SPheno`. We have also checked that the values obtained are compatible with the $\pm 3\sigma$ of the recent results from the LHCb collaboration [83].

- $\mu \rightarrow e\gamma$ and $\mu \rightarrow eee$

We have also included in our analysis the constraints from $\text{BR}(\mu \rightarrow e\gamma) < 4.2 \times 10^{-13}$ [84] and $\text{BR}(\mu \rightarrow eee) < 1.0 \times 10^{-12}$ [85], as obtained with `SPheno`.

- Chargino mass bound

In R -parity conserving (RPC) SUSY, the lower bound on the lightest chargino mass of about 94 GeV depends on the spectrum of the model [3, 35]. Although in the $\mu\nu$ SSM there is RPV and therefore this constraint does not apply automatically, we have chosen in our analysis a conservative limit of $m_{\tilde{\chi}_1^\pm} > 92$ GeV.

In addition, depending on the different masses and orderings of the lightest SUSY particles of the spectra found in our scan, we expect different signals at colliders. Besides, depending on the values of the $\mu\nu$ SSM parameters, the decay of the LSP can be prompt or displaced. Altogether, there is a variety of possible signals arising from the regions of the parameter space analyzed, that we will be able to constrain using the LHC searches of Refs. [29, 32, 86]. We will discuss these searches in detail in the next subsection.

2.3 LHC searches

The different masses and orderings of the lightest SUSY particles of the spectra found in our analysis of the $\mu\nu$ SSM parameter space can be classified in four cases:

i) LH muon-sneutrino $\tilde{\nu}_\mu$ is the LSP

When $\tilde{\nu}_\mu$ is the LSP its main decay channel corresponds to neutrinos [57, 58, 60], which constitute an invisible signal. Limits on sneutrino LSP from mono-jet and mono-photon searches have been discussed in the context of the $\mu\nu$ SSM in Refs. [58, 60], and they turn out to be ineffective to constrain it. However, the presence of charginos and neutralinos in

the spectrum with masses not far above the LSP mass is important for multi-lepton+MET searches. The relevant signals arise from the production of wino/higgsino-like chargino pairs at the LHC, which can give rise to $2\mu + 4\nu$ as shown in Fig. 2. These processes produce a signal similar to the one expected from a directly produced pair of smuons decaying as $\tilde{\mu} \rightarrow \mu + \tilde{\chi}^0$ in RPC models. Therefore, they can be compared with the limits obtained by the ATLAS collaboration in the search for sleptons in events with two leptons + MET [29].

Other decay modes are possible for the wino-like charginos, in particular chains involving higgsinos when $M_2 > \mu$. We have also considered the signals produced in events where two higgsino-like neutralinos are directly produced and decay into two smuons plus two muons, giving rise to a final signal with $4\mu + \text{MET}$. This signal can be compared with the ATLAS search for SUSY in events with four or more leptons [30]. In this scenario, we have also considered the search for events with 2 leptons + MET [29] or 3 leptons + MET [31], in the case where one or two of the muons would remain undetected. As discussed in Ref. [1], all these types of events cannot constrain our parameter space.

There is a small number of points where the LH muon-sneutrino is the LSP and the RH smuon is slightly heavier. For those points, the events initiated by RH smuon pair can produce a significant number of events including leptons and missing transverse energy, however the energy of the final states is going to be too small to produce constraints.

ii) Bino-like neutralino \tilde{B}^0 is the LSP and $\tilde{\nu}_\mu$ is the NLSP

\tilde{B}^0 can be the LSP, with $\tilde{\nu}_\mu$ lighter than wino-like chargino/neutralino and higgsino-like chargino/neutralino and therefore the next-to-LSP (NLSP), i.e. $m_{\tilde{B}^0} < m_{\tilde{\nu}_\mu} < m_{\tilde{W}, \tilde{H}}$, where we denote both \tilde{W}^\pm and \tilde{W}^0 (\tilde{H}^\pm and \tilde{H}^0) generically as \tilde{W} (\tilde{H}). Then, the proton-proton collisions produce a pair chargino-chargino, chargino-neutralino or neutralino-neutralino as shown in Fig. 3. The charginos and neutralinos will rapidly decay to sneutrinos/smuons and muons/neutrinos, with the former subsequently decaying to neutrinos/muons plus binos. When $m_{\tilde{B}^0} \lesssim m_W$ (with m_W denoting the mass of the W boson), \tilde{B}^0 decay is suppressed in comparison with the one of $\tilde{\nu}_\mu$ LSP. This originates in the kinematical suppression associated with the three-body nature of the \tilde{B}^0 decay. For this reason, it is natural that the \tilde{B}^0 proper decay length is an order of magnitude larger than the one of $\tilde{\nu}_\mu$, being therefore of the order of ten centimeters. The points of the parameter space where the LSP decays with a proper decay distance larger than 1 mm can be constrained applying the limits on long-lived particles (LLPs) obtained by the ATLAS 8 TeV search [32]. Let us point out that we have used this search instead of the more recent 13 TeV one [33], because it tests all the possible decay channels of \tilde{B}^0 while the latter focuses exclusively on leptonic displaced vertices. The conclusion is that no points of our parameter space can be excluded by the most recent analysis.

When $m_{\tilde{B}^0} \gtrsim 130$ GeV the two-body nature of its decay implies that its decay length, $c\tau$, becomes smaller than 1 mm. In that case, following the strategy discussed in Ref. [1] we can apply ATLAS searches [29] based on the promptly produced leptons in the decay of the heavier chargino-neutralino.

We have also considered here, and in *(iii)* (see below), whether the case of the direct production of a smuon pair, smuon-sneutrino or a sneutrino pair, with the smuon/sneutrino decaying into a muon/neutrino and a long lived \tilde{B}^0 , could produce a significant signal, as shown in Fig. 4. The number of events predicted in this way is added to the events produced

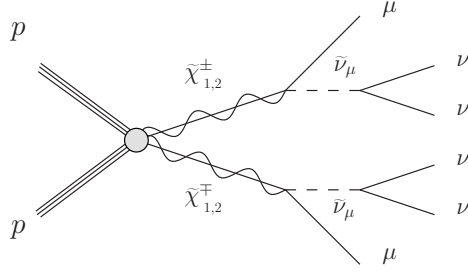


Figure 2: Production of a chargino pair, each decaying to a LH muon-sneutrino, which in turn decays to neutrinos, giving rise to the signal $2\mu + \text{MET}$.

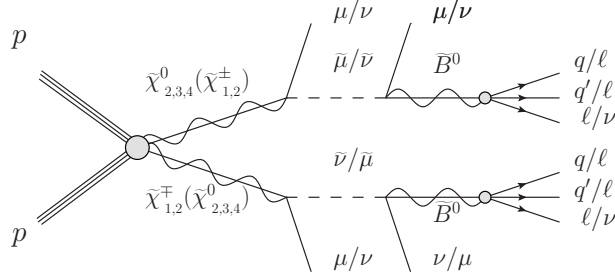


Figure 3: Production of a chargino pair, chargino-neutralino or a neutralino pair, each decaying to a LH muon-sneutrino or smuon, which in turn decay to a long-lived bino-like neutralino giving rise to a displaced signal.

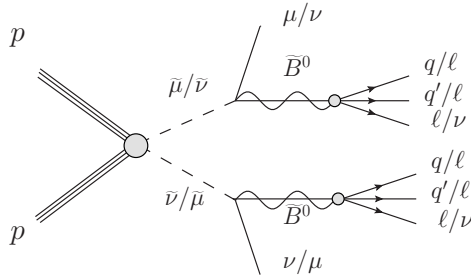


Figure 4: Production of a smuon pair, smuon-sneutrino or a sneutrino pair, each decaying to a long-lived bino-like neutralino giving rise to a displaced signal.

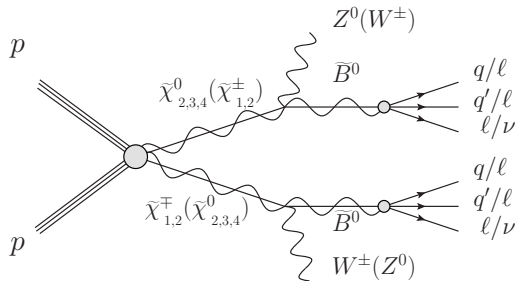


Figure 5: Production of a chargino pair, chargino-neutralino or a neutralino pair, each decaying to a long-lived bino-like neutralino giving rise to a displaced signal.

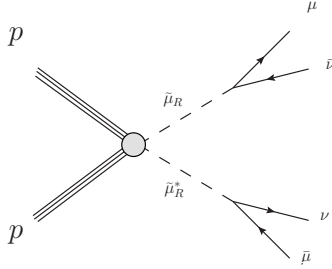


Figure 6: Production of RH smuon pair, each decaying to a RH muon and neutrino, giving rise to the signal $2\mu + \text{MET}$.

as shown in Fig. 3, and the result is that the combination of both signals excludes some points of the parameter space which are not excluded analyzing each signal separately.

iii) \tilde{B}^0 is the LSP and \tilde{W} or \tilde{H} are co-NLSPs

The situation in this case with $m_{\tilde{B}^0} < m_{\tilde{W}, \tilde{H}} < m_{\tilde{\nu}_\mu}$ is similar to the one presented in (ii), with the difference in the particles produced in the intermediate decay, as shown in Fig. 5. While before, this corresponded in most cases to muons, now the intermediate decay will mainly produce hadrons. The LHC constraints are applied in an analogous way, depending also on the value of the proper decay length, larger or smaller than 1 mm.

iv) RH smuon $\tilde{\mu}_R$ is the LSP

When $\tilde{\mu}_R$ is the LSP the limits from LEP [87–92] exclude masses smaller than 96.3 GeV for any value of its lifetime. For the rest of the points with larger values of the mass we study the following process at the LHC: once produced $\tilde{\mu}_R$ decays to a muon and a neutrino mediated by the small bino composition of the latter in the mass basis, as shown in Fig. 6. When $\tilde{\mu}_R$ decay is sufficiently suppressed to yield a proper decay length larger than 3 mm, it is constrained by the search for displaced leptons at ATLAS [86]. This search is able to constrain $\tilde{\mu}_R$ up to a mass of 500 GeV. We impose the limits that are extracted from Fig. 11d of the auxiliary material of Ref. [93]. On the contrary, if the decay of $\tilde{\mu}_R$ is fast enough to be considered prompt, it can be constrained using the search for EW production of sleptons decaying into final states with two leptons and missing transverse momentum [29]. This search imposes a lower limit of 450 GeV on the mass of $\tilde{\mu}_R$. Note that if the decay length of $\tilde{\mu}_R$ is too long to be analyzed as prompt, but shorter than 3 mm, the LHC searches are not able to put limits on its mass.

It is worth noting here that when $\tilde{\mu}_R$ is heavier than other SUSY particles, there can be three situations of interest. In one of them, \tilde{B}^0 is the LSP and $\tilde{\mu}_R$ is the NLSP. Then, the decay of $\tilde{\mu}_R$ will produce a signal similar to the one shown in Fig. 3, but without the presence of neutrinos coming from the first step of the decay. This signal can be treated therefore in a similar way, now considering the production cross-section of a $\tilde{\mu}_R$. Another situation occurs when $\tilde{\nu}_\mu$ is the LSP and $\tilde{\mu}_R$ the NLSP. The dominant decay chain in this case is $\tilde{\mu}_R \rightarrow W(\rightarrow l + \nu) + \tilde{\nu}_\mu(\rightarrow \nu\nu)$, which is similar to the one analyzed in Ref. [29] (see their Fig. 1a). Finally, we can have $\tilde{\nu}_\mu$ as the LSP, \tilde{B}^0 as the NLSP, and $\tilde{\mu}_R$ slightly heavier than both of them. In this case, the dominant $\tilde{\mu}_R$ decay chain is $\tilde{\mu}_R \rightarrow \tilde{B}^0 + \mu \rightarrow \nu + \tilde{\nu}_\mu(\rightarrow \nu\nu) + \mu$, and this signal is similar to the one analyzed in Ref. [29] (see their Fig. 1b). We conclude

that the limits for a $\tilde{\mu}_R$ heavier than the LSP, imposed as described above, do not exclude any additional point.

3 Parameter analysis

We describe in this section the methodology that we have employed to search for points of the parameter space of the $\mu\nu$ SSM that are compatible with the given experimental data. To carry out this analysis we will follow the same strategy as in Ref. [1]. This consists of combining a scan of the relevant parameters to obtain acceptable points, with a subsequent intelligent search to increase the number of points obtained. It is worth noting here that we will not perform any statistical interpretation of the set of points obtained, i.e. the `Multinest` algorithm is just used to obtain viable points.

The Higgsino mass parameter μ is important in our analysis, since it is one of the parameters controlling the SUSY contributions to a_μ as discussed in Sec. 2.1. Besides, since higgsinos have a mass of order μ , its value has also important implications for the analysis of the LHC constraints discussed in Sec. 2.3. Thus, in order to have an idea of how $a_\mu^{\mu\nu\text{SSM}}$ varies with μ , it is interesting to use two representative values of this parameter in our computation. In particular, we will use a moderate value $\mu \approx 380$ GeV, and a large value $\mu \approx 800$ GeV.

1) Moderate $\mu \approx 380$ GeV

We will perform as a *first step* a scan, using the fewest possible parameters in order to relax our demanding computing task. Here it should be noted that the most crucial parameters for neutrino physics (9) are basically decoupled from those controlling Higgs physics (12). Thus, for a suitable scan of Y_{ν_i} , v_i , M_1 and M_2 reproducing neutrino physics, there is still enough freedom to reproduce in addition Higgs data by playing with concrete values of λ , κ , $\tan\beta$, v_R , etc., as shown in Refs. [60, 1]. For $\tan\beta$ we will consider a narrow range of possible values compatible with Higgs physics. On the other hand, LH sneutrino masses $m_{\tilde{\nu}_i}$, introduce in addition the parameters T_{ν_i} (see Eq. (13)). In particular, T_{ν_2} is the most relevant one for our discussion of a low $m_{\tilde{\nu}_\mu}$, and we will scan it in an appropriate range of small values. Since the LH sneutrinos of the other two generations can be heavier, we can fix $T_{\nu_{1,3}}$ to a larger value.

Summarizing, in our first step we will perform a scan over the 9 parameters Y_{ν_i} , v_i , T_{ν_2} , $\tan\beta$, M_2 , as shown in Table 1. Concerning M_1 , we will assume for the EW gauginos $M_1 = M_2/2$. This relation is inspired by GUTs, where the low-energy result $M_2 = (\alpha_2/\alpha_1)M_1 \simeq 2M_1$ is obtained, with $g_2 = g$ and $g_1 = \sqrt{5/3} g'$. The ranges of v_i and Y_{ν_i} are natural in the context of the EW scale seesaw of the $\mu\nu$ SSM [60, 1]. The range of T_{ν_2} is chosen to have light $\tilde{\nu}_\mu$ below about 800 GeV. This is a reasonable upper bound to be able to have sizable SUSY contributions to a_μ . In the supergravity framework where $T_{\nu_2} = A_{\nu_2}Y_{\nu_2}$, this implies $-A_{\nu_2} \in (1, 4 \times 10^4)$ GeV.

Other benchmark parameters relevant for Higgs physics are fixed to appropriate values, as shown in Table 1. We choose a small/moderate value for $\lambda \approx 0.1$, thus we are in a similar situation as in the MSSM and moderate/large values of $\tan\beta$, $|T_{u_3}|$, and scalar top masses are necessary to obtain through loop effects the correct SM-like Higgs mass [61–64]. To avoid the chargino mass bound of RPC SUSY, this value of λ forces us to choose a moderate/large value of v_R to obtain a large enough value of μ (see Eq. (7)). We choose

Parameters	Scan
$\tan \beta$	(10, 16)
Y_{ν_i}	$(10^{-8}, 10^{-6})$
v_i	$(10^{-6}, 10^{-3})$
$-T_{\nu_2}$	$(10^{-6}, 4 \times 10^{-4})$
M_2	(150, 1000)
λ	0.102
κ	0.4
v_R	1750
T_λ	340
$-T_\kappa$	390
$-T_{u_3}$	4140
$m_{\tilde{Q}_{3L}}$	2950
$m_{\tilde{u}_{3R}}$	1140
$m_{\tilde{e}_{2R}}$	1000
$m_{\tilde{e}_{1,3R}}$	1000
$m_{\tilde{Q}_{1,2L}}, m_{\tilde{u}_{1,2R}}, m_{\tilde{d}_{1,2,3R}}$	1000
M_3	2700
$T_{u_{1,2}}$	0
$T_{d_{1,2}}, T_{d_3}$	0, 100
$T_{e_{1,2}}, T_{e_3}$	0, 40
$-T_{\nu_{1,3}}$	10^{-3}

Table 1: Low-energy values of the input parameters in the scan discussed in Case (1) of the text. Soft SUSY-breaking parameters and vevs are given in GeV.

$v_R = 1750$ GeV giving rise to $\mu = 378.7$ GeV. Thus in our scan the value of μ is fixed, as discussed above. Another parameter controlling the SUSY contributions to a_μ is $m_{\tilde{e}_{2R}}$ (see Eq. (15)), and we fix it in the scan to the large value $m_{\tilde{e}_{2R}} = 1000$ GeV. The parameters κ and T_κ are crucial to determine the mass scale of the RH sneutrinos. We choose $T_\kappa = -390$ GeV to have heavy pseudoscalar RH sneutrinos (of about 1190 GeV), and therefore the value of κ has to be large enough in order to avoid too light (even tachyonic) scalar RH sneutrinos. Choosing $\kappa = 0.4$, we get masses for the latter of about 700 GeV – 755 GeV. This value of κ (and the one chosen above for v_R) also implies that the Majorana mass is fixed to $\mathcal{M} = 989.9$ GeV. The parameter T_λ is relevant to obtain the correct values of the off-diagonal terms of the mass matrix mixing the RH sneutrinos with Higgses, and we choose for its value 340 GeV. The values of the parameters shown below the RH smuon mass $m_{\tilde{e}_{2R}} (\equiv m_{\tilde{\mu}_R})$ in Table 1 concern slepton, squark and gluino masses, as well as quark and lepton trilinear parameters, which are not specially relevant for our analysis of a_μ . The values chosen for $T_{\nu_{1,3}}$ are larger than the one of T_{ν_2} , but they are natural within the supergravity framework where $T_{\nu_{1,3}} = A_{\nu_{1,3}} Y_{\nu_{1,3}}$, since then larger values of the Yukawa couplings are required for similar values of A_{ν_i} . This allows us to reproduce the normal ordering of neutrino masses with $Y_{\nu_2} < Y_{\nu_1} < Y_{\nu_3}$ [60, 1]. In a similar way, the values of T_{d_3} and T_{e_3} have been chosen taking into account the corresponding Yukawa couplings.

The *second step* of our analysis of the $\mu\nu$ SMS parameter space, consists of using suitable points from the previous scan, varying appropriately some of their associated parameters in order to explore other regions, where the new points still fulfill the experimental constraints. In particular, note that in fact neutrino physics depends mainly on the parameter M defined in Eq. (8). This implies that for a given value of M reproducing the correct neutrino (and Higgs) physics, one can get different pairs of values of M_1 and M_2 with the same good properties, without essentially modifying the values of the other parameters. This allows us to break the GUT-inspired relation $M_2 = 2M_1$, to explore other interesting regions of the parameter space. On the other hand, given the value of $m_{\tilde{\nu}_\mu}$ obtained for each point, one can find more suitable points but with a different mass just varying T_{ν_2} , since this parameter does not affect the neutrino (and Higgs) physics. In addition, one can also lower the soft RH smuon mass, which leads to an enhancement of $a_\mu^{\mu\nu\text{SMS}}$ as discussed in Sec. 2.1.

2) Large $\mu \approx 800$ GeV

Although the value of μ used above is reasonable, many other values reproducing the correct Higgs physics can be obtained [63], and in particular larger ones. Thus we have also studied points with $\lambda = 0.126$, similar to the value above, but with a larger value for the vev $v_R = 3000$ GeV giving rise to $\mu = 801.9$ GeV. Other benchmark parameters relevant for Higgs physics have to be modified, such as $\kappa = 0.36$ yielding $\mathcal{M} \approx 1527.4$ GeV, $-T_\kappa = 150$ GeV, $T_\lambda = 1000$ GeV, $-T_{u_3} = 4375$ GeV, $m_{\tilde{Q}_{3L}, \tilde{u}_{3R}} = 2500$ GeV and $M_3 = 3500$ GeV. For the other squarks masses and the slepton masses we use $m_{\tilde{Q}_{1,2L}}, m_{\tilde{u}_{1,2R}}, m_{\tilde{d}_{1,2,3R}}, m_{\tilde{e}_{1,2,3R}} = 1500$ GeV. We have also modified the range of $\tan\beta$ with respect to the one in Table 1, using $\tan\beta \in (25, 35)$. Concerning the LH muon-sneutrino mass, we have slightly increased the upper limit of $-T_{\nu_2}$ up to 4.4×10^{-4} GeV, and to obtain slightly smaller chargino masses we have decreased the lower limit of M_2 up to 100 GeV. The rest of the parameters are taken as in Table 1.

Unlike the previous Case (1), instead of starting with a scan we simplify our analysis choosing several benchmark points with correct Higgs and neutrino physics, and apply to

them the variation of relevant parameters discussed in the second step above. In particular, for a given M we vary M_1 and M_2 , and for a given $m_{\tilde{\nu}_\mu}$ we vary T_{ν_2} . Obviously, more acceptable points could have been obtained with a scan, but as we will see in the next section the ones obtained are sufficient to have a good idea of the interesting regions of the $\mu\nu$ SSM parameter space when μ is large.

4 Results

We present here the results obtained following the strategy discussed in the previous section. In particular, we use the new combined $(g-2)_\mu$ result at the $\pm 2\sigma$ level to obtain upper (and lower) bounds on the EW SUSY masses. We denote the points in different regions of the parameter space, and surviving certain constraints, with different colors and symbols as shown in Figs. 7 and 8. Concerning the colors, they denote the regions where the points are located in the $\mu\nu$ SSM parameter space, as well as their agreement with the new world average of a_μ^{exp} specifying if they are in the 1σ or 2σ regions of Δa_μ in Eq. (5):

- Dark-green (1σ) and dark-blue (2σ) points correspond to Case (1) of the previous section with $m_{\tilde{e}_{2R}} = 1000$ GeV.
- Light-green (1σ) and light-blue (2σ) points are obtained from the dark-green ones but using $m_{\tilde{e}_{2R}} = 100, 150, 200, 300, 500$ GeV.
- Orange (2σ) points correspond to Case (2) of the previous section with $m_{\tilde{e}_{2R}} = 1500$ GeV.

In addition, each point surviving LHC searches can be classified in the four categories discussed in Subsec. 2.3, depending on the different relevant signals that it produces at colliders. We use the following symbols:

- i)* Dots (\circ) are points with $\tilde{\nu}_\mu$ LSP
- ii)* Crosses ($+$) are points with \tilde{B}^0 LSP and the hierarchy $m_{\tilde{B}^0} < m_{\tilde{\nu}_\mu} < m_{\tilde{W}, \tilde{H}}$
- iii)* Triangles (\triangle) are points with \tilde{B}^0 LSP and the hierarchy $m_{\tilde{B}^0} < m_{\tilde{W}, \tilde{H}} < m_{\tilde{\nu}_\mu}$
- iv)* Stars (\star) are points with $\tilde{\mu}_R$ LSP

We show in Fig. 7 the preferred parameter ranges in the $M_2 - m_{\tilde{\nu}_\mu}$ plane. As one can see, significant regions of the parameter space of the $\mu\nu$ SSM can be found being compatible with the experimental results from neutrino and Higgs measurements, as well as with flavor observables, and fulfilling the constraints from the LHC Run 1 and 2, as discussed in Sec. 2.2 and 2.3. In particular, they are in agreement with the new world average for a_μ^{exp} . LH muon-sneutrino masses are found in the range $120 \text{ GeV} \lesssim m_{\tilde{\nu}_\mu} \lesssim 540 \text{ GeV}$, and $202 \text{ GeV} \lesssim M_2 \lesssim 560 \text{ GeV}$. These values of M_2 correspond to wino-like chargino/neutralino masses in the range $200 \text{ GeV} \lesssim m_{\tilde{W}} \lesssim 597 \text{ GeV}$. The corresponding values of M_1 compatible with neutrino physics are smaller than M_2 , and they are in the range $117 \text{ GeV} \lesssim M_1 \lesssim 378 \text{ GeV}$. The range of bino-like neutralino masses is therefore $114 \text{ GeV} \lesssim m_{\tilde{B}^0} \lesssim 370 \text{ GeV}$.

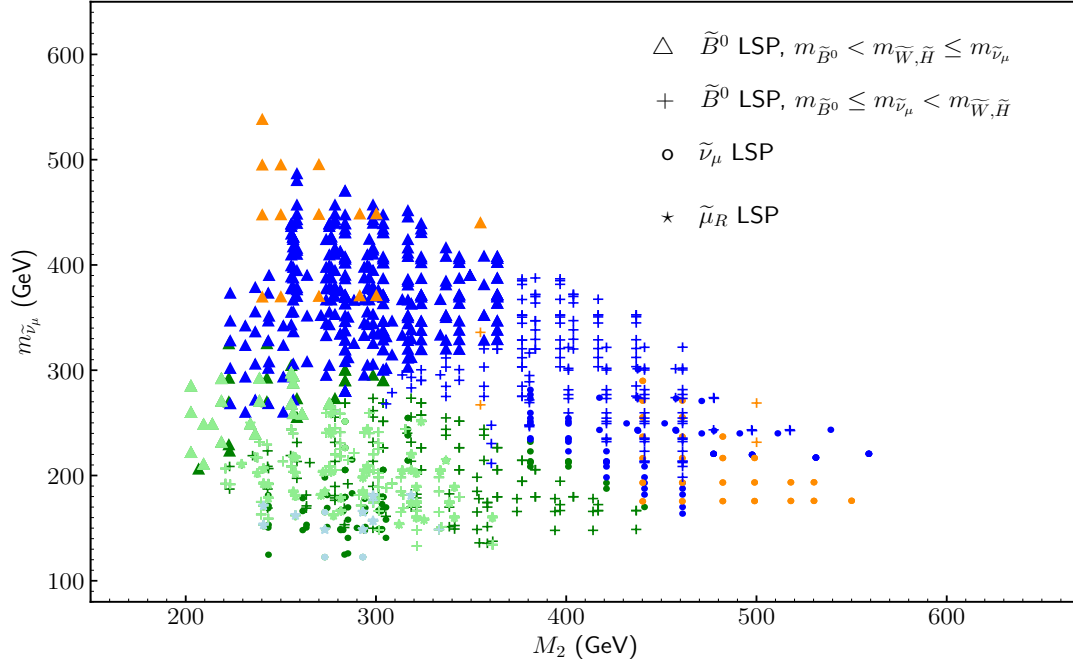


Figure 7: $m_{\tilde{\nu}_\mu}$ versus M_2 for points in the parameter space of the $\mu\nu$ SSM in agreement with the experimental constraints.

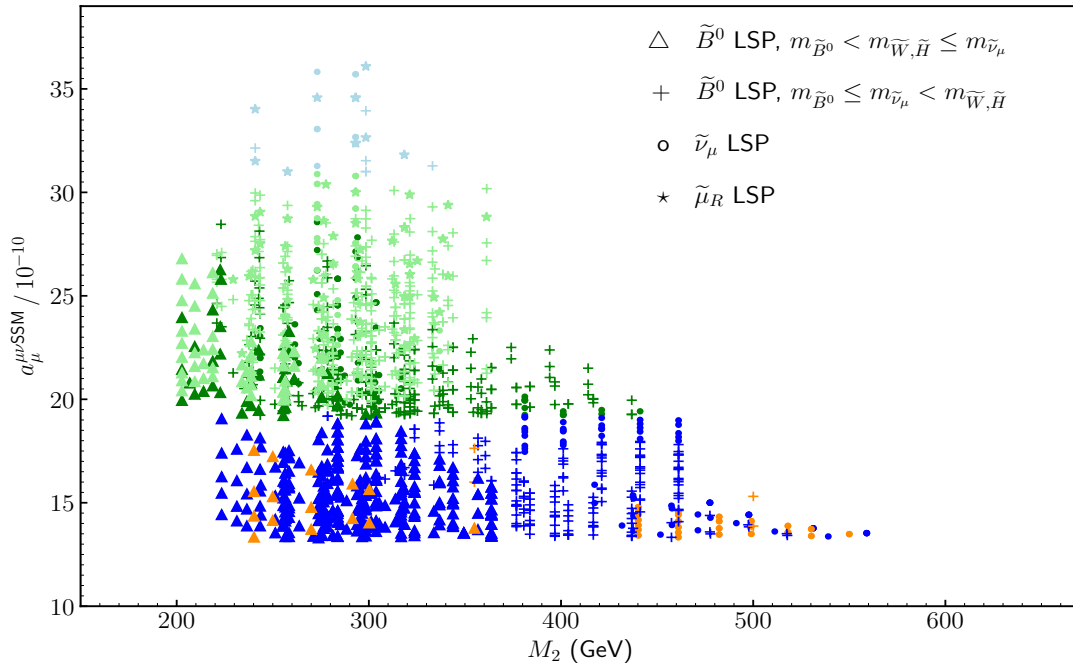


Figure 8: The same as in Fig. 7, but showing $a_{\mu}^{\mu\nu\text{SSM}}$ versus M_2 .

In Fig. 8, we show as complementary information $a_{\mu}^{\mu\nu\text{SSM}}$ versus M_2 . As we can see from both figures, the smaller M_2 ($m_{\tilde{\nu}_\mu}$) is, the larger $a_{\mu}^{\mu\nu\text{SSM}}$ becomes as expected. One can also see that the orange points with a large value of μ ($= 801.9$ GeV) do not enter

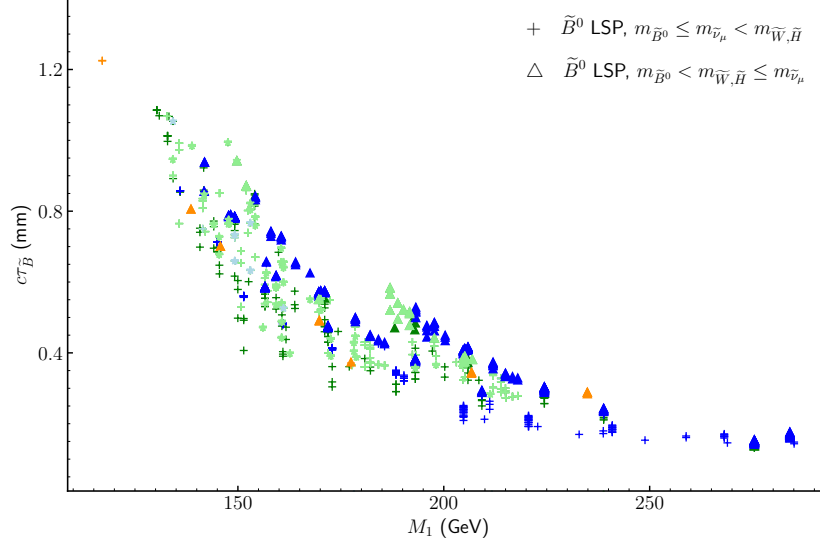


Figure 9: Proper decay length of the bino LSP $c\tau_{\tilde{B}^0}$ versus M_1 .

in the 1σ region of Δa_μ , unlike the dark- and light-green points with $\mu = 378.7$ GeV. As mentioned above, we have also analyzed how the $a_\mu^{\mu\nu\text{SSM}}$ values obtained can be enhanced lowering the value of $m_{\tilde{\mu}_R}$. In particular, we have focused on the dark-green points of the figures, which are in the 1σ region of Δa_μ , using instead of $m_{\tilde{e}_{2R}} = 1000$ GeV lower values. These points are shown in light green and light blue in Figs. 7 and 8. As one can see in the two figures, many light-green and light-blue points with an increased neutralino-smuon contribution are found with larger values for $a_\mu^{\mu\nu\text{SSM}}$. The maximum value of $a_\mu^{\mu\nu\text{SSM}}$ can be as large as about 36×10^{-10} for $m_{\tilde{e}_{2R}} = 150$ GeV. This is to be compared with the maximum value of about 29×10^{-10} obtained with $m_{\tilde{e}_{2R}} = 1000$ GeV for the dark-green points.

An interesting result of our analysis is that although LHC Runs 1 and 2 are important to constrain the $\mu\nu\text{SSM}$ scenario, it is not in fact difficult to find regions where many points are viable as well as compatible with Δa_μ , as shown in the figures. For example, a significant number of points fulfilling the experimental constraints discussed in Sec. 2.2 turn out to be forbidden by the LHC constraints discussed in Sec. 2.3. This is the case for many points with \tilde{B}^0 as the LSP, denoted by crosses and triangles. They are excluded when the GUT-inspired relation $M_2 = 2M_1$ is used. This happens for decay lengths larger as well as smaller than 1 mm, applying the displaced and prompt LHC constraints discussed in items (ii) and (iii) of Sec. 2.3. Nevertheless, the situation changes a lot allowing $M_2 \neq 2M_1$, when many of these points turn out to be unconstrained by LHC searches. All of this kind of points in Figs. 7 and 8 have $117 \text{ GeV} \lesssim M_1 \lesssim 285 \text{ GeV}$ corresponding to a proper decay length of \tilde{B}^0 LSP in the range $0.1 \text{ mm} \lesssim c\tau_{\tilde{B}^0} \lesssim 1.25 \text{ mm}$, as shown in Fig. 9.

Similarly, the light-green and light-blue stars corresponding to points with $\tilde{\mu}_R$ as the LSP with masses $106 \text{ GeV} \lesssim m_{\tilde{\mu}_R} \lesssim 190 \text{ GeV}$, have a decay length in the range $1.5 \text{ mm} \lesssim c\tau_{\tilde{\mu}_R} \lesssim 3 \text{ mm}$, avoiding in this way the LEP and LHC constraints discussed in item (iv) of Sec. 2.3.

Furthermore, more $\tilde{\nu}_\mu$ LSP-like points are allowed when a larger set of $\tilde{\nu}_\mu$ masses are explored varying T_{ν_2} for given values of the rest of parameters.

It is worth noting here that a significant number of $\tilde{\nu}_\mu$ LSP-like points are forbidden because of the limits imposed on the higgsino-like chargino pair production. This can be avoided when the presence of Binors with masses between the charginos and the LSP open new decay channels. In this situation, the signal is divided into different channels that individually don't exceed the experimental limits. These points are shown in Figs. 7 and 8 with dots, and light- and dark-green colors. Another way to avoid it is the following. Forbidding dots can occur when $M_2 > \mu$ and therefore the higgsino is lighter than the wino. Since in our scan we fixed $\mu \approx 380$ GeV, points with $M_2 \gtrsim 380$ GeV have this hierarchy of masses. Nevertheless, using a larger value of $\mu \approx 800$ GeV allows events initiated by higgsinos to pass the selection cuts. These points are shown in Figs. 7 and 8 with dots, and orange colors.

Concerning the above presented analysis the following should be kept in mind. The values of the free parameters found in agreement with the new a_μ data can be considered as a subset of all the solutions that could be obtained if a general scan of the parameter space of the model was carried out. We could have obtained straightforwardly other values for $\tan\beta$, $Y_{\nu_{ij}}$, λ , κ , v_i , v_R , etc., fulfilling all experimental constraints. Nevertheless, we do not expect significant modifications with respect to the viable intervals of the values of $m_{\tilde{\nu}_\mu}$ and M_2 shown in Fig. 7, since they correspond to the sensible regions of these parameters which can give rise to a large enough $a_\mu^{\mu\nu\text{SSM}}$.

5 Implications for future collider searches

As we have seen in the previous section, the parameter points compatible with the new world average for a_μ predict light sleptons and/or gauginos, which can be the prime target for the future (HL-)LHC experiments. Generically speaking, such light EW SUSY particles have already been stringently restricted by the existing LHC results, especially by the multi-lepton + MET searches [29–31]. Nevertheless, the parameter points shown above in the 1σ region of Δa_μ evade these limits thanks to (a) metastability of the LSP such as points with triangles, crosses and stars, or (b) close mass spectrum such as points with dots. The importance of mass degeneracy for some of the points may be inferred from the results given in Ref. [1], where both the GUT-inspired relation, $M_2 = 2M_1$, and $M_2 \neq 2M_1$ cases were analyzed; for $M_2 = 2M_1$, most of the parameter points that induce a sizable value of $a_\mu^{\mu\nu\text{SSM}}$ have already been excluded by the LHC experiments, while we can find many allowed points with $M_2 \neq 2M_1$. A part of the allowed points in Figs. 7 and 8 will be probed in the future multi-lepton + MET searches at the (HL-)LHC, and the rest of them may be explored at a larger hadron collider such as a 100 TeV collider. For the prospects of the electroweak gaugino/slepton searches at the HL-LHC (a 100 TeV collider), see Refs. [94,95] (Refs. [96–98]).

Sleptons and gauginos are more efficiently probed at lepton colliders, such as the ILC [99–101] and the CLIC [100,102], through the pair production of these particles. For the previous studies on the role of lepton colliders in testing the SUSY explanation for Δa_μ in the MSSM, see Refs. [42,43,103]. Here usually masses up to the kinematic limit, i.e. $m \lesssim \sqrt{s}/2$ for pair production, can be probed, see Ref. [104]. This covers compressed spectra as well as possibly meta-stable particles. As obtained from Fig. 7, in the present scenario, the masses of the EW SUSY particles are predicted to be $\gtrsim 114$ GeV and only a

limited parameter space is accessible to the ILC-250. Nevertheless, most of the $1\text{-}\sigma$ points can be probed with a higher energy, such as the ILC-500, CLIC Stage 1 (350/380 GeV), or FCC- ee , and the rest of the points shown in Fig. 7 may be covered at the 1-TeV ILC and CLIC Stage 2 (1.5 TeV). In addition to these electron-positron colliders, a muon collider [105–107] is also useful to discover new physics contributing to Δa_μ [108–111], since the colliding muons directly couple to it. At a muon collider, not only the EW charged states—smuons, muon sneutrinos, winos, and higgsinos—but also binos can directly be produced through the t -channel smuon exchange. This direct bino production process is useful to determine the mass and lifetime of the bino in the case of the bino LSP, which then allows us to test the characteristic prediction for their correlation, as seen in Fig. 9. We can also carry out a similar analysis for the $\tilde{\mu}_R$ LSP. A detailed study on the implications of future lepton colliders on the $\mu\nu$ SSM will be performed on another occasion.

In addition to the direct searches discussed above, we may probe our scenario in a more indirect manner. For example, the presence of light particles that couple to the Higgs bosons generically deviates the couplings of the SM-like Higgs boson from the SM prediction, and thus we can probe such signature through the precision measurements of the Higgs couplings. However, for this work we chose the parameters such that to obtain a SM-like Higgs rather similar to the SM one, producing a deviation in the Higgs coupling fairly small; for instance, the change in the Higgs-photon (Higgs-muon) coupling is found to be $\lesssim 0.8\%$ (0.2%), which is (far) below the sensitivity of the future precision Higgs measurements [101]. It is, therefore, important to pursue an option for a high-energy future collider that is capable of directly producing the EW particles with a mass of $\gtrsim 114$ GeV.

Light sleptons and/or gauginos are also predicted in the parameter region of the MSSM where the new world average for a_μ can be explained (for recent studies that discuss the SUSY explanation for Δa_μ in the MSSM based on the BNL result, see, for instance, Refs. [42, 43, 112–125, 68]). Thus, a discovery of such an electroweakly charged state by itself cannot distinguish our scenario from the MSSM explanation. We note, however, that in the case of the MSSM, the parameter regions in which sleptons are lighter than charginos are less favored (although not totally excluded, see Refs. [42, 43]) by the LHC Run 2 results [68], while such a mass spectrum is still relatively unconstrained in the $\mu\nu$ SSM. Furthermore, in the $\mu\nu$ SSM, sleptons can even be lighter than bino thanks to the R -parity violation, which is not allowed in the MSSM. We, therefore, envision that the determination of the mass spectrum of sleptons and gauginos may allow us to discriminate the $\mu\nu$ SSM from the MSSM. On the other hand, the RH sneutrinos as well as the LH sneutrinos from the first and third generation were chosen to be heavy and thus do not play a role here.

Displaced-vertex searches in the LHC Run 3 or the HL-LHC offer another promising way to cover large parts of the favored parameter space, since the presence of a metastable LSP is a characteristic prediction in the $\mu\nu$ SSM. As we discussed above, the parameter points corresponding to the cross and triangle symbols in Figs. 7 and 8 predict a metastable bino, whose decay can be observed as a displaced decay vertex. The points shown in these figures avoid the current bound from the displaced vertex search [32] since the decay length of the bino LSP is rather short, $\lesssim 1.25$ mm, as seen in Fig. 9. We note, however, that it is possible to improve the sensitivity of the displaced-vertex searches for a sub-millimeter decay length; given the extremely low background in these searches, we can safely relax the requirements on the impact parameter of lepton tracks and the reconstructed position of displaced vertices, as discussed in Ref. [58]. The decay length of the bino-

like neutralino LSP in our model is predicted to be larger than 0.1 mm [1] (see Fig. 9), which is sufficiently larger than the resolution of the transverse impact parameter, $\sigma(d_0)$ (for instance, $\sigma(d_0) \simeq 0.03$ mm for $p_T \gtrsim 10$ GeV [126]). For the parameter points corresponding to the light-green stars, on the other hand, $\tilde{\mu}_R$ LSP gives rise to the displaced-lepton signature. The sensitivity of the current search [86] is limited by the requirement on the transverse impact parameter, $|d_0| > 3$ mm, which makes it insensitive to $\tilde{\mu}_R$ with $c\tau \lesssim 3$ mm. As we mentioned above, the decay length of $\tilde{\mu}_R$ is predicted to be in the range $1.5 \text{ mm} \lesssim c\tau \lesssim 3 \text{ mm}$, and thus lowering the condition on $|d_0|$ by a factor of 2 – 3 may be sufficient to investigate the $\tilde{\mu}_R$ LSP scenario. We, therefore, strongly recommend the LHC experiments to seriously consider the optimization of the displaced-vertex/displaced lepton searches for the sub-millimeter decay length.

6 Conclusions

The EW sector of the $\mu\nu$ SSM can account for a variety of experimental data, most importantly it can account for the long-standing discrepancy of a_μ , while being in agreement with current searches at the LHC. The new result for the Run 1 data of the MUON G-2 experiment confirmed the deviation from the SM prediction found previously at BNL. Under the assumption that the previous experimental result on a_μ is uncorrelated with the new MUON G-2 result, we combined the data and obtained a new deviation from the SM prediction of $\Delta a_\mu = (25.1 \pm 5.9) \times 10^{-10}$, corresponding to a 4.2σ discrepancy. We used this new result to set limits on the $\mu\nu$ SSM parameter space.

We showed that the $\mu\nu$ SSM can naturally produce light LH muon-sneutrinos and electroweak gauginos, that are consistent with Higgs and neutrino data as well as with flavor observables such as B and μ decays. The presence of these light sparticles in the spectrum is known to enhance the chargino-sneutrino SUSY contribution to a_μ , and thus it is crucial for accommodating the discrepancy between experimental and SM values. In addition, we showed that the presence of light RH smuons increasing the neutralino-smuon contribution is helpful to obtain larger values for a_μ . We found large regions of the parameter space with these characteristics.

We applied the constraints from LHC searches on the solutions obtained. The latter have a rich collider phenomenology with the possibilities of LH muon-sneutrino, bino-like neutralino or RH smuon as LSPs. In particular, we found that multi-lepton + MET searches [29, 32, 86] can probe regions of our scenario through the production of a chargino pair, chargino-neutralino or a neutralino pair, as well as through the production of a smuon pair, smuon-sneutrino or a sneutrino pair, as shown in Figs. 2–6.

Overall we found significant regions of the parameter space of the $\mu\nu$ SSM compatible with the world average of a_μ at the 2σ level and all experimental collider data, as shown in Figs. 7 and 8. They correspond to the ranges $202 \text{ GeV} \lesssim M_2 \lesssim 560 \text{ GeV}$, $117 \text{ GeV} \lesssim M_1 \lesssim 378 \text{ GeV}$ and $150 \text{ GeV} \lesssim m_{\tilde{e}_{2R}} \lesssim 1500 \text{ GeV}$, where these values of the low-energy soft SUSY-breaking parameters imply that bino-like neutralino masses are in the range $114 \text{ GeV} \lesssim m_{\tilde{B}^0} \lesssim 370 \text{ GeV}$, wino-like chargino/neutralino masses $200 \text{ GeV} \lesssim m_{\tilde{W}} \lesssim 597 \text{ GeV}$, and RH smuon masses $106 \lesssim m_{\tilde{\mu}_R} \lesssim 1387 \text{ GeV}$. The corresponding LH muon-sneutrino masses are in the range $120 \lesssim m_{\tilde{\nu}_\mu} \lesssim 540 \text{ GeV}$. Note that the upper bounds for M_1 and $m_{\tilde{\mu}_R}$ are an artifact of our scanning setup. Larger values of these parameters

are possible, and they would only affect the small neutralino-smuon contribution to a_μ . Concerning the value of μ , we used the discrete values ≈ 380 GeV, 800 GeV, corresponding to higgsino-like chargino/neutralino masses in the range $333 \text{ GeV} \lesssim m_{\tilde{H}} \lesssim 878 \text{ GeV}$.

Finally, we discussed the implications of our results for future collider searches. As summarized in the previous paragraph, our results pin down the masses of the EW SUSY particles, and since they are predicted to be rather light, many of the allowed points in Figs. 7 and 8 can be probed in the future multi-lepton + MET searches at the (HL-)LHC. The rest of the points will be probed at a future high energy collider, such as a 100-TeV collider, the 1-TeV ILC, and the CLIC. Displaced-vertex searches in the future (HL-)LHC experiments offer another promising way to probe large parts of the favored parameter space and to test our scenario against the MSSM explanations, since the presence of a metastable LSP is a characteristic prediction in the $\mu\nu$ SSM. Many points in these figures correspond to bino LSP (crosses and triangles) or RH sneutrino LSP (stars), whose decays can be observed as a displaced decay vertex or displaced leptons, respectively. To search for these metastable particles efficiently, it is important to optimize the search strategy such that a sub-millimeter displaced vertex and ~ 1 mm displaced lepton tracks can be detected. We highly encourage the ATLAS and CMS collaborations to consider this optimization seriously.

Acknowledgments

The work of S.H. is supported in part by the MEINCOP Spain under contract PID2019-110058GB-C21 and in part by the AEI through the grant IFT Centro de Excelencia Severo Ochoa SEV-2016-0597. The research of E.K. and C.M. was supported by the AEI through grants FPA2015-65929-P (MINECO/FEDER, UE), PGC2018-095161-B-I00 and IFT Centro de Excelencia Severo Ochoa SEV-2016-0597. The work of EK was funded by the IFT SEV-2016-0597 and Proyecto Interno UAM-125. The work of I.L. was funded by the Norwegian Financial Mechanism 2014-2021, grant DEC-2019/34/H/ST2/00707. The work of D.L. was supported by the Argentinian CONICET, and also acknowledges the support through PIP 11220170100154CO. The work of N.N. was supported in part by the Grant-in-Aid for Young Scientists (No.21K13916), Innovative Areas (No.18H05542), and Scientific Research B (No.20H01897). S.H., E.K., I.L., C.M. and D.L. also acknowledge the support of the Spanish Red Consolider MultiDark FPA2017-90566-REDC.

References

- [1] E. Kpatcha, I. Lara, D. E. López-Fogliani, C. Muñoz, and N. Nagata, “Explaining muon $g - 2$ data in the $\mu\nu$ SSM,” *Eur. Phys. J. C* **81** no. 2, (2021) 154, [arXiv:1912.04163 \[hep-ph\]](#).
- [2] **Muon g-2** Collaboration, G. Bennett *et al.*, “Final Report of the Muon E821 Anomalous Magnetic Moment Measurement at BNL,” *Phys. Rev. D* **73** (2006) 072003, [arXiv:hep-ex/0602035](#).
- [3] **Particle Data Group** Collaboration, M. Tanabashi *et al.*, “Review of Particle Physics,” *Phys. Rev. D* **98** no. 3, (2018) 030001.

- [4] T. Aoyama *et al.*, “The anomalous magnetic moment of the muon in the Standard Model,” *Phys. Rept.* **887** (2020) 1–166, [arXiv:2006.04822 \[hep-ph\]](#).
- [5] A. Keshavarzi, D. Nomura, and T. Teubner, “ $g - 2$ of charged leptons, $\alpha(M_Z^2)$, and the hyperfine splitting of muonium,” *Phys. Rev. D* **101** no. 1, (2020) 014029, [arXiv:1911.00367 \[hep-ph\]](#).
- [6] M. Davier, A. Hoecker, B. Malaescu, and Z. Zhang, “A new evaluation of the hadronic vacuum polarisation contributions to the muon anomalous magnetic moment and to $\alpha(m_Z^2)$,” *Eur. Phys. J. C* **80** no. 3, (2020) 241, [arXiv:1908.00921 \[hep-ph\]](#). [Erratum: *Eur.Phys.J.C* 80, 410 (2020)].
- [7] T. Aoyama, M. Hayakawa, T. Kinoshita, and M. Nio, “Tenth-Order QED Contribution to the Electron $g-2$ and an Improved Value of the Fine Structure Constant,” *Phys. Rev. Lett.* **109** (2012) 111807, [arXiv:1205.5368 \[hep-ph\]](#).
- [8] T. Aoyama, T. Kinoshita, and M. Nio, “Theory of the Anomalous Magnetic Moment of the Electron,” *Atoms* **7** no. 1, (2019) 28.
- [9] A. Czarnecki, W. J. Marciano, and A. Vainshtein, “Refinements in electroweak contributions to the muon anomalous magnetic moment,” *Phys. Rev. D* **67** (2003) 073006, [arXiv:hep-ph/0212229](#). [Erratum: *Phys.Rev.D* 73, 119901 (2006)].
- [10] C. Gnendiger, D. Stöckinger, and H. Stöckinger-Kim, “The electroweak contributions to $(g - 2)_\mu$ after the Higgs boson mass measurement,” *Phys. Rev. D* **88** (2013) 053005, [arXiv:1306.5546 \[hep-ph\]](#).
- [11] M. Davier, A. Hoecker, B. Malaescu, and Z. Zhang, “Reevaluation of the hadronic vacuum polarisation contributions to the Standard Model predictions of the muon $g - 2$ and $\alpha(m_Z^2)$ using newest hadronic cross-section data,” *Eur. Phys. J. C* **77** no. 12, (2017) 827, [arXiv:1706.09436 \[hep-ph\]](#).
- [12] A. Keshavarzi, D. Nomura, and T. Teubner, “Muon $g - 2$ and $\alpha(M_Z^2)$: a new data-based analysis,” *Phys. Rev. D* **97** no. 11, (2018) 114025, [arXiv:1802.02995 \[hep-ph\]](#).
- [13] G. Colangelo, M. Hoferichter, and P. Stoffer, “Two-pion contribution to hadronic vacuum polarization,” *JHEP* **02** (2019) 006, [arXiv:1810.00007 \[hep-ph\]](#).
- [14] M. Hoferichter, B.-L. Hoid, and B. Kubis, “Three-pion contribution to hadronic vacuum polarization,” *JHEP* **08** (2019) 137, [arXiv:1907.01556 \[hep-ph\]](#).
- [15] A. Kurz, T. Liu, P. Marquard, and M. Steinhauser, “Hadronic contribution to the muon anomalous magnetic moment to next-to-next-to-leading order,” *Phys. Lett. B* **734** (2014) 144–147, [arXiv:1403.6400 \[hep-ph\]](#).
- [16] K. Melnikov and A. Vainshtein, “Hadronic light-by-light scattering contribution to the muon anomalous magnetic moment revisited,” *Phys. Rev. D* **70** (2004) 113006, [arXiv:hep-ph/0312226](#).

- [17] P. Masjuan and P. Sanchez-Puertas, “Pseudoscalar-pole contribution to the $(g_\mu - 2)$: a rational approach,” *Phys. Rev. D* **95** no. 5, (2017) 054026, [arXiv:1701.05829 \[hep-ph\]](#).
- [18] G. Colangelo, M. Hoferichter, M. Procura, and P. Stoffer, “Dispersion relation for hadronic light-by-light scattering: two-pion contributions,” *JHEP* **04** (2017) 161, [arXiv:1702.07347 \[hep-ph\]](#).
- [19] M. Hoferichter, B.-L. Hoid, B. Kubis, S. Leupold, and S. P. Schneider, “Dispersion relation for hadronic light-by-light scattering: pion pole,” *JHEP* **10** (2018) 141, [arXiv:1808.04823 \[hep-ph\]](#).
- [20] A. Gérardin, H. B. Meyer, and A. Nyffeler, “Lattice calculation of the pion transition form factor with $N_f = 2 + 1$ Wilson quarks,” *Phys. Rev. D* **100** no. 3, (2019) 034520, [arXiv:1903.09471 \[hep-lat\]](#).
- [21] J. Bijnens, N. Hermansson-Truedsson, and A. Rodríguez-Sánchez, “Short-distance constraints for the HLbL contribution to the muon anomalous magnetic moment,” *Phys. Lett. B* **798** (2019) 134994, [arXiv:1908.03331 \[hep-ph\]](#).
- [22] G. Colangelo, F. Hagelstein, M. Hoferichter, L. Laub, and P. Stoffer, “Longitudinal short-distance constraints for the hadronic light-by-light contribution to $(g - 2)_\mu$ with large- N_c Regge models,” *JHEP* **03** (2020) 101, [arXiv:1910.13432 \[hep-ph\]](#).
- [23] T. Blum, N. Christ, M. Hayakawa, T. Izubuchi, L. Jin, C. Jung, and C. Lehner, “Hadronic Light-by-Light Scattering Contribution to the Muon Anomalous Magnetic Moment from Lattice QCD,” *Phys. Rev. Lett.* **124** no. 13, (2020) 132002, [arXiv:1911.08123 \[hep-lat\]](#).
- [24] G. Colangelo, M. Hoferichter, A. Nyffeler, M. Passera, and P. Stoffer, “Remarks on higher-order hadronic corrections to the muon $g-2$,” *Phys. Lett. B* **735** (2014) 90–91, [arXiv:1403.7512 \[hep-ph\]](#).
- [25] **Muon g-2** Collaboration, J. Grange *et al.*, “Muon (g-2) Technical Design Report,” [arXiv:1501.06858 \[physics.ins-det\]](#).
- [26] **Muon g-2** Collaboration, C. Polly, “Talk: First results from the Muon $g - 2$ experiment at Fermilab,” (April 7, 2021) .
- [27] D. E. López-Fogliani and C. Muñoz, “Proposal for a supersymmetric standard model,” *Phys. Rev. Lett.* **97** (2006) 041801, [arXiv:hep-ph/0508297 \[hep-ph\]](#).
- [28] D. E. Lopez-Fogliani and C. Munoz, “Searching for Supersymmetry: The $\mu\nu$ SSM,” *Eur. Phys. J. ST* **229** no. 21, (2020) 3263–3301, [arXiv:2009.01380 \[hep-ph\]](#).
- [29] **ATLAS** Collaboration, G. Aad *et al.*, “Search for electroweak production of charginos and sleptons decaying into final states with two leptons and missing transverse momentum in $\sqrt{s} = 13$ TeV pp collisions using the ATLAS detector,” *Eur. Phys. J. C* **80** no. 2, (2020) 123, [arXiv:1908.08215 \[hep-ex\]](#).

- [30] **ATLAS** Collaboration, M. Aaboud *et al.*, “Search for supersymmetry in events with four or more leptons in $\sqrt{s} = 13$ TeV pp collisions with ATLAS,” *Phys. Rev. D* **98** no. 3, (2018) 032009, [arXiv:1804.03602](#) [hep-ex].
- [31] **ATLAS** Collaboration, M. Aaboud *et al.*, “Search for electroweak production of supersymmetric particles in final states with two or three leptons at $\sqrt{s} = 13$ TeV with the ATLAS detector,” *Eur. Phys. J. C* **78** no. 12, (2018) 995, [arXiv:1803.02762](#) [hep-ex].
- [32] **ATLAS** Collaboration, G. Aad *et al.*, “Search for massive, long-lived particles using multitrack displaced vertices or displaced lepton pairs in pp collisions at $\sqrt{s} = 8$ TeV with the ATLAS detector,” *Phys. Rev.* **D92** no. 7, (2015) 072004, [arXiv:1504.05162](#) [hep-ex].
- [33] **ATLAS** Collaboration, G. Aad *et al.*, “Search for displaced vertices of oppositely charged leptons from decays of long-lived particles in pp collisions at $\sqrt{s} = 13$ TeV with the ATLAS detector,” *Phys. Lett. B* **801** (2020) 135114, [arXiv:1907.10037](#) [hep-ex].
- [34] **CMS** Collaboration, A. M. Sirunyan *et al.*, “Search for supersymmetry in final states with two oppositely charged same-flavor leptons and missing transverse momentum in proton-proton collisions at $\sqrt{s} = 13$ TeV,” [arXiv:2012.08600](#) [hep-ex].
- [35] **CMS** Collaboration, A. M. Sirunyan *et al.*, “Combined search for electroweak production of charginos and neutralinos in proton-proton collisions at $\sqrt{s} = 13$ TeV,” *JHEP* **03** (2018) 160, [arXiv:1801.03957](#) [hep-ex].
- [36] **CMS** Collaboration, S. Chatrchyan *et al.*, “Search in Leptonic Channels for Heavy Resonances Decaying to Long-Lived Neutral Particles,” *JHEP* **02** (2013) 085, [arXiv:1211.2472](#) [hep-ex].
- [37] H. P. Nilles, “Supersymmetry, Supergravity and Particle Physics,” *Phys. Rept.* **110** (1984) 1–162.
- [38] R. Barbieri, “Looking Beyond the Standard Model: The Supersymmetric Option,” *Riv. Nuovo Cim.* **11N4** (1988) 1–45.
- [39] H. E. Haber and G. L. Kane, “The Search for Supersymmetry: Probing Physics Beyond the Standard Model,” *Phys. Rept.* **117** (1985) 75–263.
- [40] J. Gunion and H. E. Haber, “Higgs Bosons in Supersymmetric Models. 1.,” *Nucl. Phys. B* **272** (1986) 1. [Erratum: *Nucl.Phys.B* 402, 567–569 (1993)].
- [41] S. P. Martin, “A Supersymmetry primer,” [arXiv:hep-ph/9709356](#) [hep-ph]. [Adv. Ser. Direct. High Energy Phys.18,1(1998)].
- [42] M. Chakraborti, S. Heinemeyer, and I. Saha, “Improved $(g - 2)_\mu$ Measurements and Supersymmetry,” *Eur. Phys. J. C* **80** no. 10, (2020) 984, [arXiv:2006.15157](#) [hep-ph].

- [43] M. Chakraborti, S. Heinemeyer, and I. Saha, “Improved $(g - 2)_\mu$ Measurements and Wino/Higgsino Dark Matter,” [arXiv:2103.13403 \[hep-ph\]](#).
- [44] M. Chakraborti, S. Heinemeyer, and I. Saha, “IFT-UAM/CSIC-21-033,” (2021) .
- [45] M. Maniatis, “The Next-to-Minimal Supersymmetric extension of the Standard Model reviewed,” *Int. J. Mod. Phys. A* **25** (2010) 3505–3602, [arXiv:0906.0777 \[hep-ph\]](#).
- [46] U. Ellwanger, C. Hugonie, and A. M. Teixeira, “The Next-to-Minimal Supersymmetric Standard Model,” *Phys. Rept.* **496** (2010) 1–77, [arXiv:0910.1785 \[hep-ph\]](#).
- [47] F. Capozzi, E. Di Valentino, E. Lisi, A. Marrone, A. Melchiorri, and A. Palazzo, “Global constraints on absolute neutrino masses and their ordering,” *Phys. Rev. D* **95** no. 9, (2017) 096014, [arXiv:1703.04471 \[hep-ph\]](#).
- [48] P. F. de Salas, D. V. Forero, C. A. Ternes, M. Tortola, and J. W. F. Valle, “Status of neutrino oscillations 2018: 3σ hint for normal mass ordering and improved CP sensitivity,” *Phys. Lett. B* **782** (2018) 633–640, [arXiv:1708.01186 \[hep-ph\]](#).
- [49] P. F. De Salas, S. Gariazzo, O. Mena, C. A. Ternes, and M. Tórtola, “Neutrino Mass Ordering from Oscillations and Beyond: 2018 Status and Future Prospects,” *Front. Astron. Space Sci.* **5** (2018) 36, [arXiv:1806.11051 \[hep-ph\]](#).
- [50] I. Esteban, M. C. Gonzalez-Garcia, A. Hernandez-Cabezudo, M. Maltoni, and T. Schwetz, “Global analysis of three-flavour neutrino oscillations: synergies and tensions in the determination of θ_{23} , δ_{CP} , and the mass ordering,” *JHEP* **01** (2019) 106, [arXiv:1811.05487 \[hep-ph\]](#).
- [51] N. Escudero, D. E. López-Fogliani, C. Muñoz, and R. R. de Austri, “Analysis of the parameter space and spectrum of the $\mu\nu$ SSM,” *JHEP* **12** (2008) 099, [arXiv:0810.1507 \[hep-ph\]](#).
- [52] P. Ghosh and S. Roy, “Neutrino masses and mixing, lightest neutralino decays and a solution to the μ problem in supersymmetry,” *JHEP* **04** (2009) 069, [arXiv:0812.0084 \[hep-ph\]](#).
- [53] A. Bartl, M. Hirsch, A. Vicente, S. Liebler, and W. Porod, “LHC phenomenology of the $\mu\nu$ SSM,” *JHEP* **05** (2009) 120, [arXiv:0903.3596 \[hep-ph\]](#).
- [54] J. Fidalgo, D. E. López-Fogliani, C. Muñoz, and R. R. de Austri, “Neutrino physics and spontaneous CP violation in the $\mu\nu$ SSM,” *JHEP* **08** (2009) 105, [arXiv:0904.3112 \[hep-ph\]](#).
- [55] P. Ghosh, P. Dey, B. Mukhopadhyaya, and S. Roy, “Radiative contribution to neutrino masses and mixing in $\mu\nu$ SSM,” *JHEP* **05** (2010) 087, [arXiv:1002.2705 \[hep-ph\]](#).

- [56] S. Liebler and W. Porod, “On-shell renormalization of neutralino and chargino mass matrices in R-parity violating models - Correlation between LSP decays and neutrino mixing angles revisited,” *Nucl. Phys. B* **855** (2012) 774–800, [arXiv:1106.2921 \[hep-ph\]](#).
- [57] P. Ghosh, I. Lara, D. E. López-Fogliani, C. Muñoz, and R. Ruiz de Austri, “Searching for left sneutrino LSP at the LHC,” *Int. J. Mod. Phys. A* **33** no. 18n19, (2018) 1850110, [arXiv:1707.02471 \[hep-ph\]](#).
- [58] I. Lara, D. E. López-Fogliani, C. Muñoz, N. Nagata, H. Otono, and R. Ruiz De Austri, “Looking for the left sneutrino LSP with displaced-vertex searches,” *Phys. Rev. D* **98** no. 7, (2018) 075004, [arXiv:1804.00067 \[hep-ph\]](#).
- [59] I. Lara, D. E. López-Fogliani, and C. Muñoz, “Electroweak superpartners scrutinized at the LHC in events with multi-leptons,” *Phys. Lett. B* **790** (2019) 176–183, [arXiv:1810.12455 \[hep-ph\]](#).
- [60] E. Kpatcha, I. , D. E. López-Fogliani, C. Muñoz, N. Nagata, H. Otono, and R. Ruiz De Austri, “Sampling the $\mu\nu$ SSM for displaced decays of the tau left sneutrino LSP at the LHC,” *Eur. Phys. J. C* **79** no. 11, (2019) 934, [arXiv:1907.02092 \[hep-ph\]](#).
- [61] T. Biekotter, S. Heinemeyer, and C. Muñoz, “Precise prediction for the Higgs-boson masses in the $\mu\nu$ SSM,” *Eur. Phys. J. C* **78** no. 6, (2018) 504, [arXiv:1712.07475 \[hep-ph\]](#).
- [62] T. Biekotter, S. Heinemeyer, and C. Muñoz, “Precise prediction for the Higgs-Boson masses in the $\mu\nu$ SSM with three right-handed neutrino superfields,” *Eur. Phys. J. C* **79** no. 8, (2019) 667, [arXiv:1906.06173 \[hep-ph\]](#).
- [63] E. Kpatcha, D. E. López-Fogliani, C. Muñoz, and R. Ruiz De Austri, “Impact of Higgs physics on the parameter space of the $\mu\nu$ SSM,” *Eur. Phys. J. C* **80** no. 4, (2020) 336, [arXiv:1910.08062 \[hep-ph\]](#).
- [64] T. Biekötter, “munuSSM: A python package for the μ -from- ν Supersymmetric Standard Model,” *Comput. Phys. Commun.* **264** (2021) 107935, [arXiv:2009.12887 \[hep-ph\]](#).
- [65] P. Ghosh, D. E. López-Fogliani, V. A. Mitsou, C. Muñoz, and R. Ruiz de Austri, “Probing the $\mu\nu$ SSM with light scalars, pseudoscalars and neutralinos from the decay of a SM-like Higgs boson at the LHC,” *JHEP* **11** (2014) 102, [arXiv:1410.2070 \[hep-ph\]](#).
- [66] T. Moroi, “The Muon anomalous magnetic dipole moment in the minimal supersymmetric standard model,” *Phys. Rev. D* **53** (1996) 6565–6575, [arXiv:hep-ph/9512396](#). [Erratum: *Phys.Rev.D* 56, 4424 (1997)].
- [67] D. G. Cerdeno, E. Gabrielli, S. Khalil, C. Munoz, and E. Torrente-Lujan, “Muon anomalous magnetic moment in supersymmetric scenarios with an intermediate scale and nonuniversality,” *Phys. Rev. D* **64** (2001) 093012, [arXiv:hep-ph/0104242 \[hep-ph\]](#).

- [68] M. Endo, K. Hamaguchi, S. Iwamoto, and T. Kitahara, “Muon $g - 2$ vs LHC Run 2 in supersymmetric models,” *JHEP* **04** (2020) 165, [arXiv:2001.11025 \[hep-ph\]](#).
- [69] F. Feroz, M. P. Hobson, and M. Bridges, “MultiNest: an efficient and robust Bayesian inference tool for cosmology and particle physics,” *Mon. Not. Roy. Astron. Soc.* **398** (2009) 1601–1614, [arXiv:0809.3437 \[astro-ph\]](#).
- [70] F. Staub, “SARAH 4 : A tool for (not only SUSY) model builders,” *Comput. Phys. Commun.* **185** (2014) 1773, [arXiv:1309.7223 \[hep-ph\]](#).
- [71] W. Porod, “SPHeno, a program for calculating supersymmetric spectra, SUSY particle decays and SUSY particle production at $e^+ e^-$ colliders,” *Comput. Phys. Commun.* **153** (2003) 275, [arXiv:hep-ph/0301101 \[hep-ph\]](#).
- [72] W. Porod and F. Staub, “SPHeno 3.1: Extensions including flavour, CP-phases and models beyond the MSSM,” *Comput. Phys. Commun.* **183** (2012) 2458–2469, [arXiv:1104.1573 \[hep-ph\]](#).
- [73] **Planck** Collaboration, N. Aghanim *et al.*, “Planck 2018 results. VI. Cosmological parameters,” *Astron. Astrophys.* **641** (2020) A6, [arXiv:1807.06209 \[astro-ph.CO\]](#).
- [74] P. Bechtle, O. Brein, S. Heinemeyer, G. Weiglein, and K. E. Williams, “HiggsBounds: Confronting Arbitrary Higgs Sectors with Exclusion Bounds from LEP and the Tevatron,” *Comput. Phys. Commun.* **181** (2010) 138, [arXiv:0811.4169 \[hep-ph\]](#).
- [75] P. Bechtle, O. Brein, S. Heinemeyer, G. Weiglein, and K. E. Williams, “HiggsBounds 2.0.0: Confronting Neutral and Charged Higgs Sector Predictions with Exclusion Bounds from LEP and the Tevatron,” *Comput. Phys. Commun.* **182** (2011) 2605, [arXiv:1102.1898 \[hep-ph\]](#).
- [76] P. Bechtle, O. Brein, S. Heinemeyer, O. Stal, T. Stefaniak, G. Weiglein, and K. E. Williams, “HiggsBounds – 4: Improved Tests of Extended Higgs Sectors against Exclusion Bounds from LEP, the Tevatron and the LHC,” *Eur. Phys. J. C* **74** no. 3, (2014) 2693, [arXiv:1311.0055 \[hep-ph\]](#).
- [77] P. Bechtle, S. Heinemeyer, O. Stal, T. Stefaniak, and G. Weiglein, “Applying Exclusion Likelihoods from LHC Searches to Extended Higgs Sectors,” *Eur. Phys. J. C* **75** no. 9, (2015) 421, [arXiv:1507.06706 \[hep-ph\]](#).
- [78] P. Bechtle, D. Dercks, S. Heinemeyer, T. Klingl, T. Stefaniak, G. Weiglein, and J. Wittbrodt, “HiggsBounds-5: Testing Higgs Sectors in the LHC 13 TeV Era,” *Eur. Phys. J. C* **80** no. 12, (2020) 1211, [arXiv:2006.06007 \[hep-ph\]](#).
- [79] P. Bechtle, S. Heinemeyer, O. Stal, T. Stefaniak, and G. Weiglein, “*HiggsSignals*: Confronting arbitrary Higgs sectors with measurements at the Tevatron and the LHC,” *Eur. Phys. J. C* **74** no. 2, (2014) 2711, [arXiv:1305.1933 \[hep-ph\]](#).

- [80] P. Bechtle, S. Heinemeyer, T. Klingl, T. Stefaniak, G. Weiglein, and J. Wittbrodt, “HiggsSignals-2: Probing new physics with precision Higgs measurements in the LHC 13 TeV era,” *Eur. Phys. J. C* **81** no. 2, (2021) 145, [arXiv:2012.09197 \[hep-ph\]](#).
- [81] **Heavy Flavor Averaging Group** Collaboration, Y. Amhis *et al.*, “Averages of B-Hadron, C-Hadron, and tau-lepton properties as of early 2012,” [arXiv:1207.1158 \[hep-ex\]](#).
- [82] **CMS, LHCb** Collaboration, “Combination of results on the rare decays $B_{(s)}^0 \rightarrow \mu^+ \mu^-$ from the CMS and LHCb experiments,”
- [83] M. Santimaria, “New results on theoretically clean observables in rare B-meson decays from LHCb,” 2021. Talk at LHC Seminar, Mar. 23, 2021.
- [84] **MEG** Collaboration, A. M. Baldini *et al.*, “Search for the lepton flavour violating decay $\mu^+ \rightarrow e^+ \gamma$ with the full dataset of the MEG experiment,” *Eur. Phys. J. C* **76** no. 8, (2016) 434, [arXiv:1605.05081 \[hep-ex\]](#).
- [85] **SINDRUM** Collaboration, U. Bellgardt *et al.*, “Search for the Decay $\mu^+ \rightarrow e^+ e^+ e^-$,” *Nucl. Phys. B* **299** (1988) 1–6.
- [86] **ATLAS** Collaboration, G. Aad *et al.*, “Search for displaced leptons in $\sqrt{s} = 13$ TeV pp collisions with the ATLAS detector,” [arXiv:2011.07812 \[hep-ex\]](#).
- [87] **ALEPH** Collaboration, A. Heister *et al.*, “Search for gauge mediated SUSY breaking topologies in $e^+ e^-$ collisions at center-of-mass energies up to 209-GeV,” *Eur. Phys. J. C* **25** (2002) 339–351, [arXiv:hep-ex/0203024](#).
- [88] **OPAL** Collaboration, G. Abbiendi *et al.*, “Searches for gauge-mediated supersymmetry breaking topologies in $e^+ e^-$ collisions at LEP2,” *Eur. Phys. J. C* **46** (2006) 307–341, [arXiv:hep-ex/0507048](#).
- [89] **DELPHI** Collaboration, J. Abdallah *et al.*, “Search for supersymmetric particles in light gravitino scenarios and sleptons NLSP,” *Eur. Phys. J. C* **27** (2003) 153–172, [arXiv:hep-ex/0303025](#).
- [90] **OPAL** Collaboration, G. Abbiendi *et al.*, “Search for anomalous production of dilepton events with missing transverse momentum in $e^+ e^-$ collisions at $\sqrt{s} = 183$ -GeV to 209-GeV,” *Eur. Phys. J. C* **32** (2004) 453–473, [arXiv:hep-ex/0309014](#).
- [91] **DELPHI** Collaboration, J. Abdallah *et al.*, “Searches for supersymmetric particles in $e^+ e^-$ collisions up to 208-GeV and interpretation of the results within the MSSM,” *Eur. Phys. J. C* **31** (2003) 421–479, [arXiv:hep-ex/0311019](#).
- [92] ALEPH, DELPHI, L3, OPAL Experiments, “Combined LEP GMSB Stau/Smuon/Selectron Results, 189-208 GeV.” [Lepsusywg/02-09.2, 2002.](#)
http://lepsusy.web.cern.ch/lepsusy/www/gmsb_summer02/lep_gmsb.html.

- [93] **ATLAS** Collaboration, “‘RH smuon upper limit on cross section’ of ‘Search for displaced leptons in $\sqrt{s} = 13$ TeV pp collisions with the ATLAS detector’,” 2020. <https://doi.org/10.17182/hepdata.98796.v1/t10>.
- [94] **ATLAS** Collaboration, “Prospects for searches for staus, charginos and neutralinos at the high luminosity LHC with the ATLAS Detector,”.
- [95] X. Cid Vidal *et al.*, “Report from Working Group 3: Beyond the Standard Model physics at the HL-LHC and HE-LHC,” *CERN Yellow Rep. Monogr.* **7** (2019) 585–865, [arXiv:1812.07831](https://arxiv.org/abs/1812.07831) [hep-ph].
- [96] S. Gori, S. Jung, L.-T. Wang, and J. D. Wells, “Prospects for Electroweakino Discovery at a 100 TeV Hadron Collider,” *JHEP* **12** (2014) 108, [arXiv:1410.6287](https://arxiv.org/abs/1410.6287) [hep-ph].
- [97] N. Arkani-Hamed, T. Han, M. Mangano, and L.-T. Wang, “Physics opportunities of a 100 TeV proton–proton collider,” *Phys. Rept.* **652** (2016) 1–49, [arXiv:1511.06495](https://arxiv.org/abs/1511.06495) [hep-ph].
- [98] T. Golling *et al.*, “Physics at a 100 TeV pp collider: beyond the Standard Model phenomena,” [arXiv:1606.00947](https://arxiv.org/abs/1606.00947) [hep-ph].
- [99] “The International Linear Collider Technical Design Report - Volume 2: Physics,” [arXiv:1306.6352](https://arxiv.org/abs/1306.6352) [hep-ph].
- [100] A. Arbey *et al.*, “Physics at the e^+e^- Linear Collider,” *Eur. Phys. J. C* **75** no. 8, (2015) 371, [arXiv:1504.01726](https://arxiv.org/abs/1504.01726) [hep-ph].
- [101] K. Fujii *et al.*, “Physics Case for the 250 GeV Stage of the International Linear Collider,” [arXiv:1710.07621](https://arxiv.org/abs/1710.07621) [hep-ex].
- [102] R. Franceschini *et al.*, “The CLIC Potential for New Physics,” [arXiv:1812.02093](https://arxiv.org/abs/1812.02093) [hep-ph].
- [103] M. Endo, K. Hamaguchi, S. Iwamoto, T. Kitahara, and T. Moroi, “Reconstructing Supersymmetric Contribution to Muon Anomalous Magnetic Dipole Moment at ILC,” *Phys. Lett. B* **728** (2014) 274–281, [arXiv:1310.4496](https://arxiv.org/abs/1310.4496) [hep-ph].
- [104] M. Berggren, “What pp SUSY limits mean for future e^+e^- colliders,” in *International Workshop on Future Linear Colliders*. 3, 2020. [arXiv:2003.12391](https://arxiv.org/abs/2003.12391) [hep-ph].
- [105] J. P. Delahaye, M. Diemoz, K. Long, B. Mansoulié, N. Pastrone, L. Rivkin, D. Schulte, A. Skrinsky, and A. Wulzer, “Muon Colliders,” [arXiv:1901.06150](https://arxiv.org/abs/1901.06150) [physics.acc-ph].
- [106] K. Long, D. Lucchesi, M. Palmer, N. Pastrone, D. Schulte, and V. Shiltsev, “Muon colliders to expand frontiers of particle physics,” *Nature Phys.* **17** no. 3, (2021) 289–292, [arXiv:2007.15684](https://arxiv.org/abs/2007.15684) [physics.acc-ph].
- [107] H. A. Ali *et al.*, “The Muon Smasher’s Guide,” [arXiv:2103.14043](https://arxiv.org/abs/2103.14043) [hep-ph].

- [108] R. Capdevilla, D. Curtin, Y. Kahn, and G. Krnjaic, “A Guaranteed Discovery at Future Muon Colliders,” [arXiv:2006.16277 \[hep-ph\]](#).
- [109] D. Buttazzo and P. Paradisi, “Probing the muon $g-2$ anomaly at a Muon Collider,” [arXiv:2012.02769 \[hep-ph\]](#).
- [110] W. Yin and M. Yamaguchi, “Muon $g - 2$ at multi-TeV muon collider,” [arXiv:2012.03928 \[hep-ph\]](#).
- [111] R. Capdevilla, D. Curtin, Y. Kahn, and G. Krnjaic, “A No-Lose Theorem for Discovering the New Physics of $(g - 2)_\mu$ at Muon Colliders,” [arXiv:2101.10334 \[hep-ph\]](#).
- [112] T. T. Yanagida and N. Yokozaki, “Muon $g - 2$ in MSSM gauge mediation revisited,” *Phys. Lett. B* **772** (2017) 409–414, [arXiv:1704.00711 \[hep-ph\]](#).
- [113] M. Endo, K. Hamaguchi, S. Iwamoto, and K. Yanagi, “Probing minimal SUSY scenarios in the light of muon $g - 2$ and dark matter,” *JHEP* **06** (2017) 031, [arXiv:1704.05287 \[hep-ph\]](#).
- [114] K. Hagiwara, K. Ma, and S. Mukhopadhyay, “Closing in on the chargino contribution to the muon $g-2$ in the MSSM: current LHC constraints,” *Phys. Rev. D* **97** no. 5, (2018) 055035, [arXiv:1706.09313 \[hep-ph\]](#).
- [115] E. Bagnaschi *et al.*, “Likelihood Analysis of the pMSSM11 in Light of LHC 13-TeV Data,” *Eur. Phys. J. C* **78** no. 3, (2018) 256, [arXiv:1710.11091 \[hep-ph\]](#).
- [116] J. C. Costa *et al.*, “Likelihood Analysis of the Sub-GUT MSSM in Light of LHC 13-TeV Data,” *Eur. Phys. J. C* **78** no. 2, (2018) 158, [arXiv:1711.00458 \[hep-ph\]](#).
- [117] G. Bhattacharyya, T. T. Yanagida, and N. Yokozaki, “An extended gauge mediation for muon $(g - 2)$ explanation,” *Phys. Lett. B* **784** (2018) 118–121, [arXiv:1805.01607 \[hep-ph\]](#).
- [118] M. E. Gómez, S. Lola, R. Ruiz De Austri, and Q. Shafi, “Dark matter, sparticle spectroscopy and muon $(g - 2)$ in $SU(4)_c \times SU(2)_L \times SU(2)_R$,” *JHEP* **10** (2018) 062, [arXiv:1806.06220 \[hep-ph\]](#).
- [119] B. Dutta and Y. Mimura, “Electron $g - 2$ with flavor violation in MSSM,” *Phys. Lett. B* **790** (2019) 563–567, [arXiv:1811.10209 \[hep-ph\]](#).
- [120] P. Cox, C. Han, T. T. Yanagida, and N. Yokozaki, “Gaugino mediation scenarios for muon $g - 2$ and dark matter,” *JHEP* **08** (2019) 097, [arXiv:1811.12699 \[hep-ph\]](#).
- [121] M. Ibe, M. Suzuki, T. T. Yanagida, and N. Yokozaki, “Muon $g - 2$ in Split-Family SUSY in light of LHC Run II,” *Eur. Phys. J. C* **79** no. 8, (2019) 688, [arXiv:1903.12433 \[hep-ph\]](#).
- [122] M. Endo and W. Yin, “Explaining electron and muon $g - 2$ anomaly in SUSY without lepton-flavor mixings,” *JHEP* **08** (2019) 122, [arXiv:1906.08768 \[hep-ph\]](#).

- [123] M. Badziak and K. Sakurai, “Explanation of electron and muon $g - 2$ anomalies in the MSSM,” *JHEP* **10** (2019) 024, [arXiv:1908.03607](#) [[hep-ph](#)].
- [124] M. Abdughani, K.-I. Hikasa, L. Wu, J. M. Yang, and J. Zhao, “Testing electroweak SUSY for muon $g - 2$ and dark matter at the LHC and beyond,” *JHEP* **11** (2019) 095, [arXiv:1909.07792](#) [[hep-ph](#)].
- [125] T. T. Yanagida, W. Yin, and N. Yokozaki, “Muon $g - 2$ in Higgs-anomaly mediation,” *JHEP* **06** (2020) 154, [arXiv:2001.02672](#) [[hep-ph](#)].
- [126] **ATLAS** Collaboration, G. Aad *et al.*, “The ATLAS Inner Detector commissioning and calibration,” *Eur. Phys. J.* **C70** (2010) 787–821, [arXiv:1004.5293](#) [[physics.ins-det](#)].